Senile plaques in Alzheimer's disease arise from Cathepsin D and Aβ-enriched proteinaceous mixtures out of hemolysis and vascular degeneration

Running title：The blood and vascular origin of senile plaques

Hualin Fu[1, 2*], Jilong Li[1], Peng Du[3], Weilin Jin[1, 2, §], Guo Gao[1, 2], Daxiang Cui[1, 2]

Affiliations:

[1] Institute of Nano Biomedicine and Engineering, Department of Instrument Science and Engineering, School of Electronic Information and Electrical Engineering, Shanghai Jiao Tong University, 800 Dongchuan Road, Shanghai, 200240, P. R. China

[2] National Center for Translational Medicine, Shanghai Jiao Tong University, 800 Dongchuan Road, Shanghai, 200240, P. R. China

[3] Department of Colorectal Surgery, Xinhua Hospital, School of Medicine, Shanghai Jiao Tong University, Shanghai, China

[§] Current address: Institute of Cancer Neuroscience, Medical Frontier Innovation Research Center, The First Hospital of Lanzhou University, The First Clinical Medical College of Lanzhou University, Lanzhou 730000, China

*Correspondence to: hfu@sjtu.edu.cn or 1010720220@qq.com (Hualin Fu)

Abstract

The senile plaque is a prominent pathological hallmark of Alzheimer's disease (AD)，yet the mechanism governing senile plaque generation remains intensively debated. Many researchers believed that senile plaques are derived from neuronal cells; however, there is also strong evidence that senile plaques are linked to cerebral microhemorrhage. We analyzed major neural markers, blood vessel and blood markers on AD brain sections with immunohistochemistry, TUNEL assay, fluorescence imaging and histochemical staining. We found little co-expression between neural markers and

plaque Aβ while abundant co-expression between blood markers such as HBA, HbA1C or ApoE and plaque Aβ. Senile plaques additionally colocalized with a characteristic blue autofluorescence, which also prominently existed in red blood cells. Moreover，platelets were found along blood vessel walls and in plaques, suggesting that platelets also contribute to senile plaque formation. Senile plaque formation was intrinsically linked to vascular degeneration as showed by ColIV, ACTA2 and LRP1 immunostaining. We found that Aβ distributes unevenly among red cells or in the blood vessels, enriching in domains of red cell damage or vascular damage, and with the presence of luminal Cathepsin D expression. In addition，the senile plaques have a constitutive Cathepsin D expression overlapping with Aβ, HBA and HbA1C, reiterating a senile plaque connection with hemolysis. With Rhodanine staining, we further proved that there is widespread hemolysis in AD brain tissues, which concurs with Aβ aggregation, Cathepsin D and ApoE expression. Moreover, we provided the biochemical evidence that Aβ directly interacts with hemoglobin (Hb) and form protease-sensitive complexes in an *in vitro* polymerization assay. In summary, our data suggested that senile plaques arise from Cathepsin D and Aβ-enriched proteinaceous mixtures out of hemolysis and vascular degeneration. In addition, hemoglobin could be a primary physiological target of Aβ in hemolysis and in senile plaques.

Keywords: senile plaque; Aβ; Cathepsin D; hemolysis; vascular degeneration；hemoglobin; Alzheimer's disease

Introduction

Alzheimer's disease has several important pathological hallmarks such as senile plaques, dystrophic neurites, neurofibillary tangles and cerebral amyloid angiopathy (CAA)[1-4]. Beta amyloid peptide (Aβ) turned out to be a major component in both senile plaques and CAA[5,6]. However, the mechanism governing Aβ generation in senile plaques and the linkage between CAA and senile plaques is still not clear. Most researchers believed that senile plaques are derived from neuronal cells as proposed in amyloid cascade

hypothesis[7,8]. On the other hand, there is also strong evidence showing that senile plaques are linked with cerebral microhemorrhage[9-18]. In depth AD mouse model studies based on bone marrow transplantation experiments also indicated that there is a clear role of hematopoietic cell Aβ contributing to senile plaque development[19]. We used immunohistochemistry, fluorescence imaging, TUNEL assay and histochemical staining to examine the neural, vascular or blood Aβ contribution to senile plaque development in AD brain tissues. We found that there is a lack of significant direct neural cell Aβ input to senile plaques. The true direct source of senile plaque Aβ appears to be Aβ-associated hemolytic red blood cells that come out of cerebral blood vessels through vascular leakage or vascular degeneration while CAA is an important intermediate stage during this senile plaque formation process.

MATERIAL AND METHODS

Tissue sections. AD patient frontal lobe brain paraffin tissue sections were purchased from GeneTex (Irvine, CA, USA). Additionally, AD patient frontal lobe brain paraffin tissue sections were provided by National Human Brain Bank for Development and Function, Chinese Academy of Medical Sciences and Peking Union Medical College, Beijing, China. This study was supported by the Institute of Basic Medical Sciences, Chinese Academy of Medical Sciences, Neuroscience Center, and the China Human Brain Banking Consortium. All procedures involving human subjects are done in accord with the ethical standards of the Committee on Human Experimentation in Shanghai Jiao Tong University and in Xinhua Hospital, and in accord with the Helsinki Declaration of 1975.

List of antibodies for immunohistochemistry. The following primary antibodies and dilutions have been used in this study: Aβ (Abcam ab201061, 1:200), Aβ/AβPP (CST #2450, 1:200), phos-TAU (Abcam ab151559, 1:200), αSyn (Proteintech 10842-1-AP,

1:200), MAP2 (Proteintech 17490-1-AP, 1:200), GFAP (Abcam ab33922， 1:200), GFAP (Proteintech 60190-1-Ig, 1:100), Iba1 (Abcam ab178847, 1:200), ColIV (Abcam ab236640, 1:200), ACTA2 (Proteintech 23081-1-AP, 1:400), LRP1 (Abcam ab92544, 1:200), ApoE (Abcam ab183597, 1:200), CD42b (Abcam ab210407, 1:200), HBA (Abcam ab92492, 1:200), Anti-Glycophorin A antibody (Abcam ab129024, 1:200), Cathepsin D (Proteintech 66534-1-Ig, 1:100), Cathepsin D (Abcam ab75852, 1:200), HbA1c (OkayBio K5a2, 1:100). The following secondary antibodies and dilutions have been used in this study: donkey anti-mouse Alexa-594 secondary antibody (Jackson ImmunoResearch 715-585-150, 1:400), donkey anti-rabbit Alexa-488 secondary antibody (Jackson ImmunoResearch 711-545-152, 1:400), donkey anti-rabbit Alexa-594 secondary antibody (Jackson ImmunoResearch 711-585-152, 1:400), and donkey anti-mouse Alexa-488 secondary antibody (Jackson ImmunoResearch 715-545-150, 1:400).

Immunohistochemistry was performed as described[20]. Briefly, paraffin sections were deparaffinized by Xylene, 100% EtOH, 95% EtOH, 75% EtOH, 50% EtOH, and PBS washes. Sections were treated with 10 mM pH6.0 sodium citrate or 10mM pH9.0 Tris-EDTA solution with microwave at high power for 3 times of 4 minutes, with 5 minutes intervals. The sections were allowed to naturally cool down to room temperature. Then, the slides were blocked with TBST 3%BSA solution for 1 hour at room temperature. After blocking, the samples were incubated with primary antibodies at room temperature for 2 hrs followed by 5 washes of TBST. After that, the samples were incubated with fluorescent secondary antibodies overnight at 4 degree. The treated samples were washed again with TBST 5 times the second day and mounted with PBS+50% glycerol supplemented with H33342 nuclear dye (Sigma, B2261, 1 μg/ml) and ready for imaging. To differentiate nuclear staining from MetaBlue autofluorescence signal, in some of the IHC experiments, PI (Sigma, P4170, 10 μg/ml) was used as a red nuclear fluorescence dye instead of H33342, which stained the nuclei with blue fluorescence. IHC experiments without primary antibodies were used as negative controls. All experiments have been repeated in order to verify the

reproducibility of the results.

TUNEL assay. TUNEL assay kits (C1089) were purchased from Beyotime Biotechnology (Shanghai, China). TUNEL assay was performed as described in the manufacturer's user manual. Briefly, paraffin sections were deparaffinized by Xylene, 100% EtOH, 95% EtOH, 75% EtOH, 50% EtOH, and H_2O washes. Then, the sections were digested with Proteinase K (20 μg/ml) in 10mM TE buffer (pH 7.5) for 15 minutes at room temperature. After Proteinase K digestion, the slides were washed with PBS for 5 times. The slides were then incubated in 50 μl freshly-prepared TUNEL labeling mixture, covered with parafilm and incubated for 1 hour at 37 degree. Afterwards, the slides were washed with PBS for 5 times and mounted with PBS+50% glycerol solution with Hoechst nuclear dye and examined under fluorescent microscopes. To perform double labeling of TUNEL and antibody staining, the incubation time of Proteinase K treatment was shortened and adjusted to allow the simultaneous detection of protein antigens and TUNEL signals.

Rhodanine staining： The Rhodanine staining kit (BA4346) was purchased from Baso Diagnostics Inc. (Zhuhai, China). Briefly, paraffin sections were first deparaffinized by Xylene, 100% EtOH, 95% EtOH, 75% EtOH, 50% EtOH, and H_2O washes. After a quick wash in 95% ethanol, the slides were stained in the Rhodanine staining solution (0.01% p-Dimethylaminobenzalrhodanine) at 37 degree for 30 minutes. After staining, the slides were treated with a 95% ethanol quick wash and 5 times wash in water, then mounted with PBS+50% glycerol solution for imaging analysis.

Slide-based Aβ aggregation assay: Human Aβ40 or Aβ42 peptides (Apeptide Co., Shanghai, China) were first solubilized with DMSO at 1 mg/mL concentration. Human hemoglobin (H7379, Sigma) was solubilized in sterile H_2O at 10 mg/mL concentration. Then, Aβ peptides were diluted into sterile PBS solution at 5μM concentration with or without 1.25 μM hemoglobin. The mixture was incubated at 37 degree up to 3 days. Samples were obtained at Day 0, Day 1, Day 2, and Day 3. 2 μl out of each obtained

sample was spotted onto adhesive glass slides and dried up in a 37-degree incubator. The glass slides with samples were fixed with 4% formaldehyde in PBS for 10 minutes at room temperature and washed 3 times with PBS. To test the sensitivity of aggregates to protease digestion, paralleled slides were treated with Proteinase K at 20 μg/mL in 10mM TE (pH 7.5) buffer for 15 minutes at room temperature. The procedure to analyze the Aβ aggregates on the slides using antibodies was the same as in immunohistochemistry.

I**maging and morphometry analysis**. Most images were taken with a Leica DM6000B microscope (Leica Microsystems, Wetzlar, Germany) with A4, L5 and N3 fluorescent filter cubes. The microscope is equipped with 10X eyepiece, and 5X, 10X, 20X, 40X objective lens. During the time of manuscript preparation, an Olympus IX71 fluorescent microscope (Olympus Co., Toyoko, Japan) was also used to examine the slides. Some additional images were taken by a Keyence BZ-X800 microscope (Keyence Co., Itasca， USA). When comparing marker immunostaining densities, identical exposure settings for fluorescent channels were used for both control and test groups. Images were then analyzed with Image J software. Mean area density was used as the parameter to define the marker densities. The areas of different structures were also measured with Image J software. The total area intensity was calculated by multiplying the area mean density with the measured area. When using the average neural cell as a reference, the values of other anatomical structures divided the mean value of neural cells to obtain the fold numbers. The folds of changes were then expressed as means with standard deviations.

Statistics. All data first went through a Shapiro & Wilk normality test using SPSS Statistics 19 software. Two-tailed unpaired T-test was used to compare the means of data with a normal distribution with Excel 2007 software. For data that were not normally distributed, nonparametric Mann/Whitney test was performed to compare the means with Megastat addin version 10.2. The p Value threshold for statistical significance is set at 0.05. If $p<0.05$, then the difference was considered statistically

178 significant. When $p<0.001$, it was labeled as $p<0.001$. If $p \geqq 0.001$, then the p Value was
179 shown as it was. "*" in the statistical figures indicated the differences are statistically
180 significant.
181
182 **Results:**
183
184 **Neural marker staining rarely overlapped with senile plaque Aβ staining**
185
186 If senile plaque Aβ comes from neural cells, theoretically, senile plaque Aβ expression
187 should overlap with some neural markers because *in vivo* Aβ does not exist as a single
188 species molecule but rather associates with many other molecules[21]. We checked the
189 expression of neuronal marker MAP2, pan-neural marker αSYN and phos-Tau,
190 astroglial marker GFAP and microglial marker Iba1 in AD patient frontal lobe brain
191 tissues. In this study, in order to get a broad image of Aβ-related changes during senile
192 plaque development, "Aβ" refer to all peptides containing the "Aβ" peptide sequence,
193 including the precursor protein AβPP. We found rare overlaps between senile plaque Aβ
194 with MAP2, αSYN and phos-Tau (Figure 1A-F) and some spotty overlaps of GFAP or
195 Iba1 with senile plaque Aβ (Figure 1G-J). Overall, there is no prominent neural marker
196 overlapping with senile plaque Aβ expression. Especially, in the center of dense-core
197 senile plaques, there is no expression of any of the neural markers that we have checked.
198 The data suggested that Aβ from other sources likely form the bulk of Aβ materials in
199 the senile plaques.
200
201 Although neural marker labeling rarely overlaps with the strong fibrillar Aβ signals in
202 senile plaques， neural cells do express Aβ related peptides at very low levels. This very
203 low level of Aβ expression in neural cells can be detected side by side with strong senile
204 plaque Aβ staining with longer exposure settings (Figure 2). In pathological specimens,
205 we observed that some senile plaques or CAA blood vessels were surrounded by a few
206 weakly-stained Aβ-positive neural cells (Figure 2A, C). However, sometimes Aβ-
207 positive neural cells were not observed in the immediate vicinity of senile plaques or

CAA blood vessels (Figure 2B, D). Neural cell Aβ staining was much weaker than in senile plaques or CAA (Figure 2E). We also observed significant Aβ staining in luminal patches of blood cells (Figure 2F-H). In order to estimate the relative contribution of Aβ to senile plaques from different sources, we quantitated the densities of Aβ staining in different compartments in the AD brain tissues (Figure 2I, J). We analyzed the mean area Aβ densities of 46 large senile plaques (for simplicity reasons, we only chose a few large senile plaques per view for this analysis), 9 CAA blood vessels, 9 blood vessel luminal Aβ-positive regions and 238 neural cells across 34 high power (40X) microscopic fields in one set of experiments with Aβ staining. The average area in luminal Aβ-positive blood cell patches, CAA and senile plaques is 44.40 (±53.63), 19.03 (±9.20), 4.97 (±2.68) fold of the area of an average Aβ-positive neural cell (Figure 2I). Comparing to the mean area intensity of Aβ in neural cells, the mean area intensity of luminal Aβ-positive blood cell patches, CAA and senile plaques is around 1.85 (±0.59), 5.59 (±0.74), 5.06 (±0.93) fold of an average neural cell (Figure 2J). The mean area Aβ intensity of CAA was not statistically different from the mean area Aβ intensity of senile plaques ($p=0.08$), while the difference between Aβ intensities of luminal Aβ-positive blood cell patches and average neural cells was statistically significant ($p<0.001$). By multiplying the average area and mean area intensity numbers，the total area intensity of Aβ in an average senile plaque is roughly 25.14 times of the total area Aβ intensity of an average neural cell. Take this estimation to the three-dimensional level, an average senile plaque approximately contains the same amount of Aβ in as many as 126.03 average neural cells (estimated by multiplying the total area intensity fold number with the square root of the total area intensity fold number). In another word, an average Aβ-positive neural cell only has about 0.79% of the Aβ content in an average senile plaque. Based on counting results from 34 high power fields, each microscopic field contained by average 2.62 (±1.99) large senile plaques while 46.94 (±9.53) Aβ-positive neural cells. When comparing to an average senile plaque, the mean area Aβ intensities of luminal patches and CAA are 0.37 (±0.12) and 1.10 (±0.15) fold of an average senile plaque. The average areas of luminal patches and CAA are 8.94 (±10.8) and 3.83 (±1.85) fold of an average senile plaque. At the three-dimensional

level, an average CAA blood vessel contains the same amount of Aβ as in roughly 8.65 average senile plaques while an average luminal Aβ-positive region contains the same amount of Aβ as in roughly 6.02 average senile plaques. The experiment was repeated on different samples and with different fluorophores and the results showed similarly the extremely low Aβ expression in neural cells comparing to senile plaques. This quantitative analysis pointed out that the very low level Aβ in neural cells and the limited number of neural cells might not provide sufficient amount of Aβ for the senile plaque formation while Aβ-positive blood cells and CAA blood vessels contained sufficient amount of Aβ, which could be the source of Aβ in senile plaques.

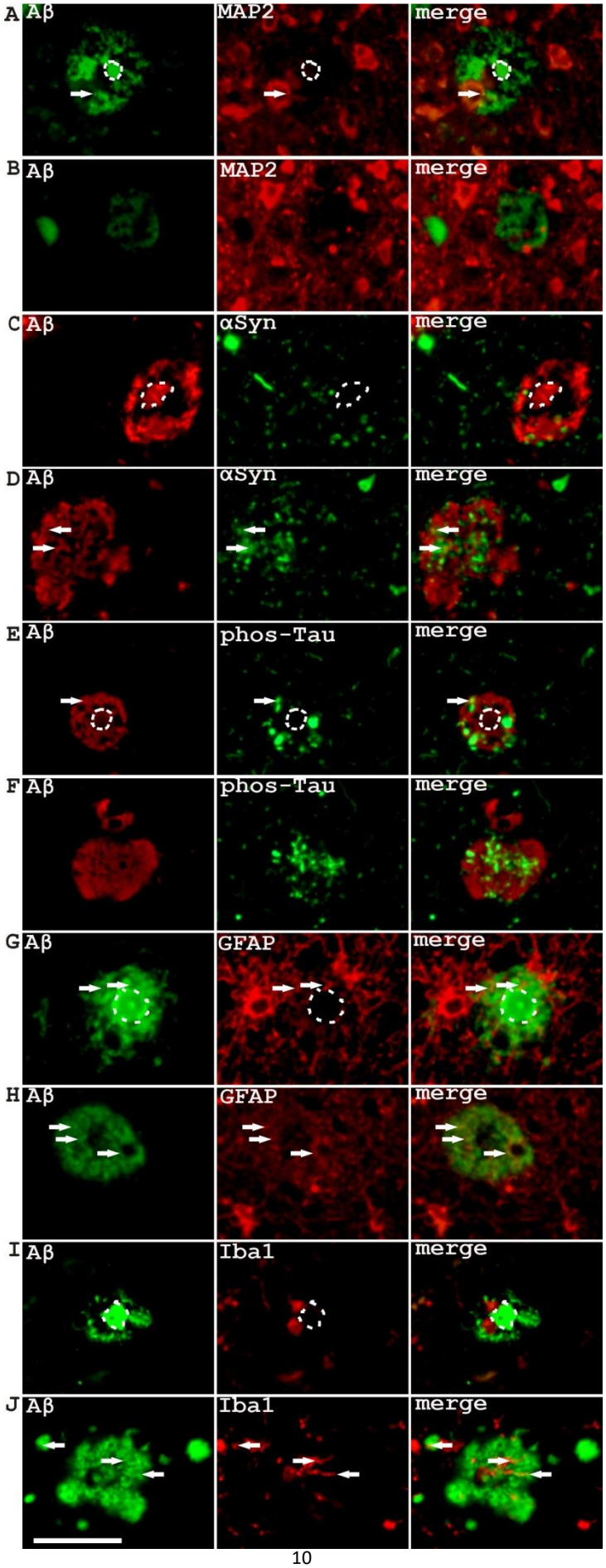

Figure 1. Co-immunostaining of neuronal marker MAP2, pan-neural markers αSYN and phos-Tau or glial cell markers GFAP and Iba1 with Aβ in dense-core (top panel for each marker) or diffusive senile plaques (bottom panel for each marker). (**A-B**), MAP2; (**C-D**), αSYN; (**E-F**), phos-Tau; (**G-H**), GFAP; (**I-J**), Iba1. Arrows pointed to possible overlapping of the markers. The circled areas indicated the core of dense-core plaques, which were not stained with any of the neural markers examined. Scale bar, 50 μm.

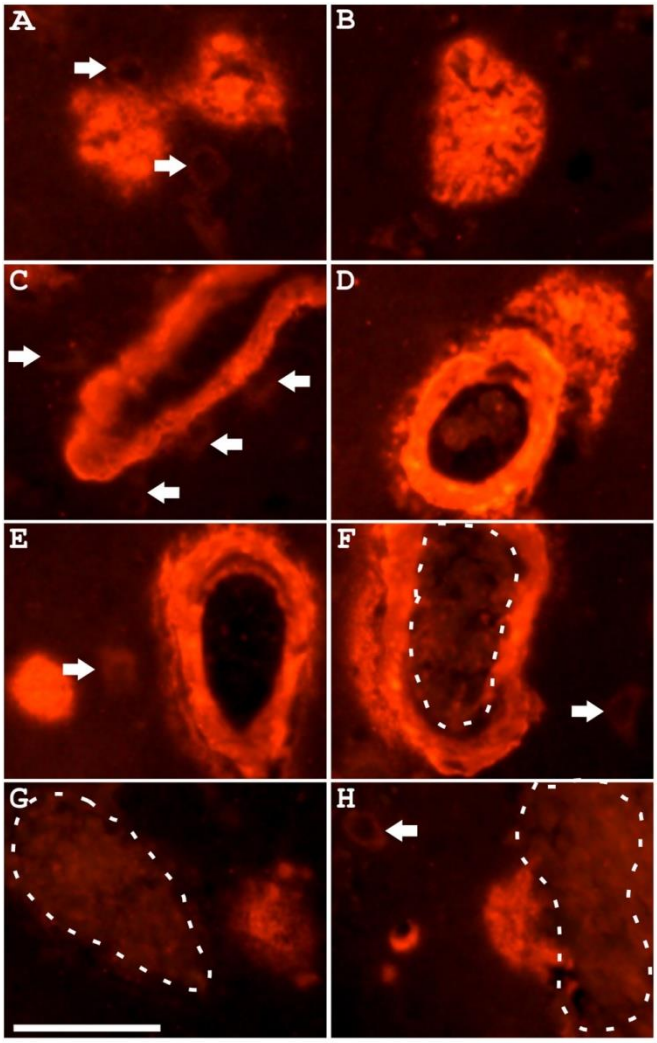

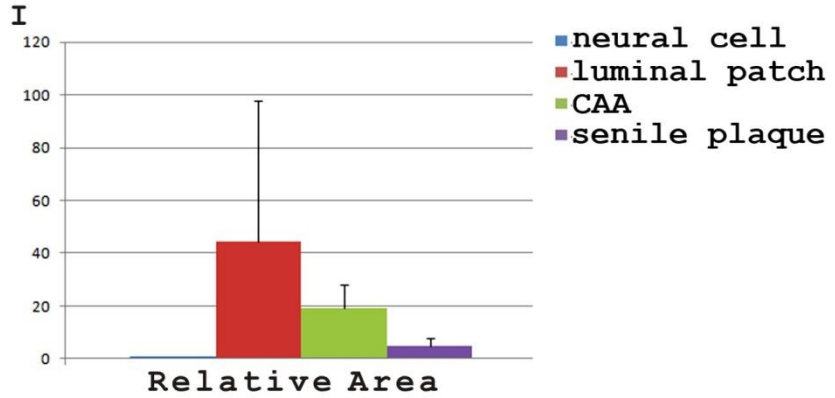

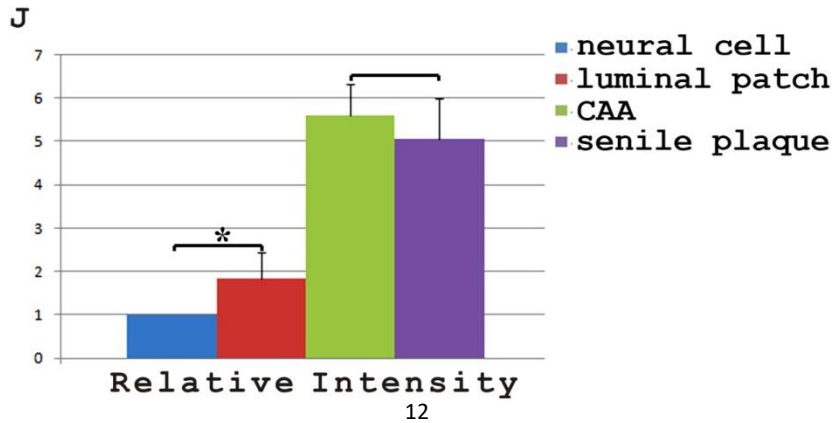

256

Figure 2. Aβ staining in neural cells, senile plaques, CAA, and luminal patch of Aβ-positive blood cells. (**A**，**B**) Senile plaques with or without weakly Aβ-positive neural cells at the vicinity. (**C**，**D**) CAA with or without weakly Aβ-positive neural cells at the vicinity. **E.** Neural cell Aβ (indicated with an arrow) staining was much weaker comparing to plaque (left) or CAA (right) Aβ staining. **F.** CAA and luminal blood cell Aβ staining was stronger than neural cell Aβ staining (indicated with an arrow). **G.** Blood cell Aβ staining (on the left) intensity was weaker comparing to a developing senile plaque (on the right). **H.** Perivascular plaque and blood cell Aβ staining (dashed lines) was stronger than neural cell Aβ staining (indicated with an arrow). The arrows indicated the weakly stained neural cells. The dashed lines indicate luminal blood cells. Scale bar, 50 μm. **I.** The average area in luminal Aβ-positive blood cell patches, CAA and senile plaques is 44.40±53.63, 19.03±9.20, 4.97±2.68 fold of the area of an average neural cell. **J.** The mean area intensity of luminal Aβ-positive blood cell patches, CAA and senile plaques is around 1.85±0.59, 5.59±0.74, 5.06±0.93 fold of an average neural cell. Aβ intensities of luminal Aβ-positive blood cell patches were significantly higher than average neural cells ($p<0.001$) while no significant difference was detected between CAA and senile plaque Aβ intensities ($p=0.08$). The asterisk indicated statistical significance.

Senile plaque Aβ staining seldom colocalized with nuclear stains

Because Aβ often showed extracellular localizations, people assumed that Aβ might be derived from dead neurons. However, the direct evidence that linked senile plaque Aβ with dying neurons is lacking. In our analysis, most Aβ plaques did not have nuclei associations, agreeing with their predominantly extracellular localizations (Figure 3A). In addition, Aβ plaques did not colocalized with TUNEL-labeled nuclei, disagreeing with the assumption that Aβ might come from dying neurons (Figure 3B). Surprisingly, we observed a faint blue fluorescent staining in the centers of many dense-core plaques, which showed amorphous irregular patterns distinct from densely-stained oval shape nucleus staining (Figure 3A, bottom). To differentiate blue autofluorescence from blue

nuclei staining, we switched to use a red fluorescence nuclei dye Propidium Iodide (PI). We proved that the amorphous blue fluorescent staining in the center of dense-core senile plaques is a blue autofluorescence, but not nuclei staining (Figure 3C). This blue autofluorescence was a robust and consistent marker of senile plaques, which associated with senile plaques of different morphologies and sizes including dense-core senile plaques, large diffusive senile plaques and small diffusive senile plaques (with more pictures shown in Supplementary Figure 1). We think the blue autofluorescent material could be a constitutive component of senile plaques that associates with Aβ during the full course of senile plaque formation process. At the time of preparing this manuscript, we noticed that several earlier studies already recognized senile plaques had characteristic autofluorescence although the true source of this blue autofluorescence is unknown[22,23]. To facilitate the study and discussion on this unique and potentially important substance, we would like to give a temporary special name for this material as "MetaBlue" in this manuscript (meaning for a blue metabolite or a mixture of blue metabolites) until the accurate identity of this material is fully revealed.

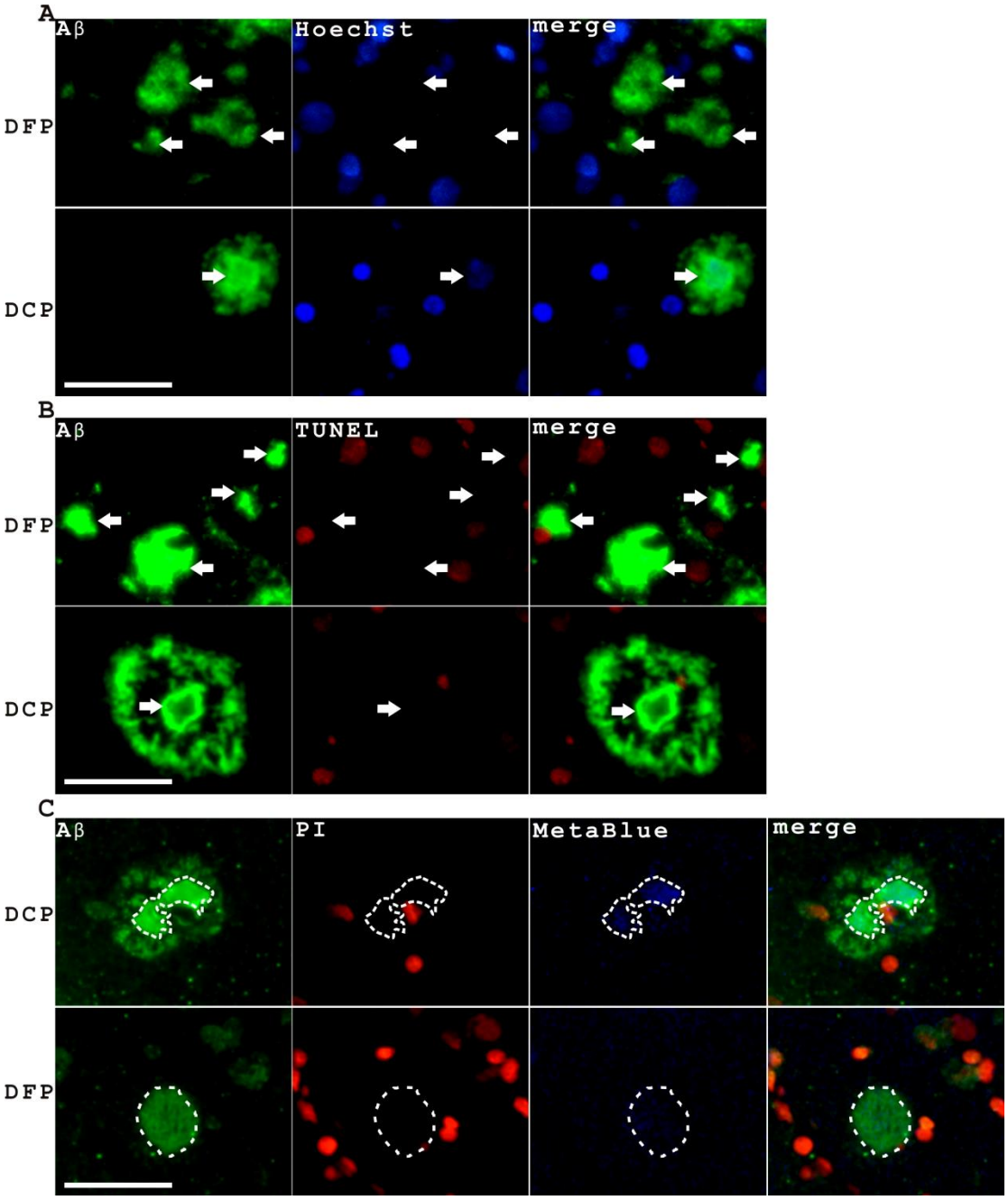

Figure 3. Senile plaques seldom associated with nuclei DNA staining. A. Senile plaques were seldom stained with Hoechst. Diffusive plaques (DFP) or stella plaques were mostly not stained with Hoechst. Irregular amorphous blue fluorescent signals were observed in the cores of dense-core plaques (DCP) but distinct from nuclear staining. Arrows point to senile plaques. **B.** Diffusive plaques (DFP) or dense-core plaques (DCP) were not associated with TUNEL-labeled nuclei. Arrows point to senile plaques. **C.** Dense-core plaques (DCP) had a relatively strong blue autofluorescence while the blue autofluorescence signal in diffusive plaques (DFP) was weak. The

dashed lines indicated dense-core or diffusive senile plaques with blue autofluorescence but without PI-positive nuclei. Scale bar, 50 μm.

Senile plaque Aβ staining overlapped with MetaBlue, a specific blue autofluorescence, that was also prominently found in red blood cells

To trace the origin of MetaBlue, we combined immunohistochemistry staining with autofluorescence imaging. We found that MetaBlue was prominently associated with Aβ (Figure 4A) and HBA (Figure 4B) in CAA blood vessel wall，senile plaques and red blood cells. The intensity of MetaBlue in the center of Aβ-marked dense-core plaques is comparable to the MetaBlue intensity in CAA blood vessels and often higher than in diffusive senile plaques, which suggested that MetaBlue is either degraded or dispersed in diffusive plaques or the diffusive plaques have less MetaBlue materials starting with. MetaBlue signals were clearly observed in red blood cells identified with HBA or Glycophorin A staining (Figure 4C). With the senile plaque association of predominantly blood origin MetaBlue and HBA but much less with neural markers such as MAP2, αSYN, phos-TAU, GFAP and Iba1, it suggested that senile plaque Aβ might directly come from the blood instead of neural cells.

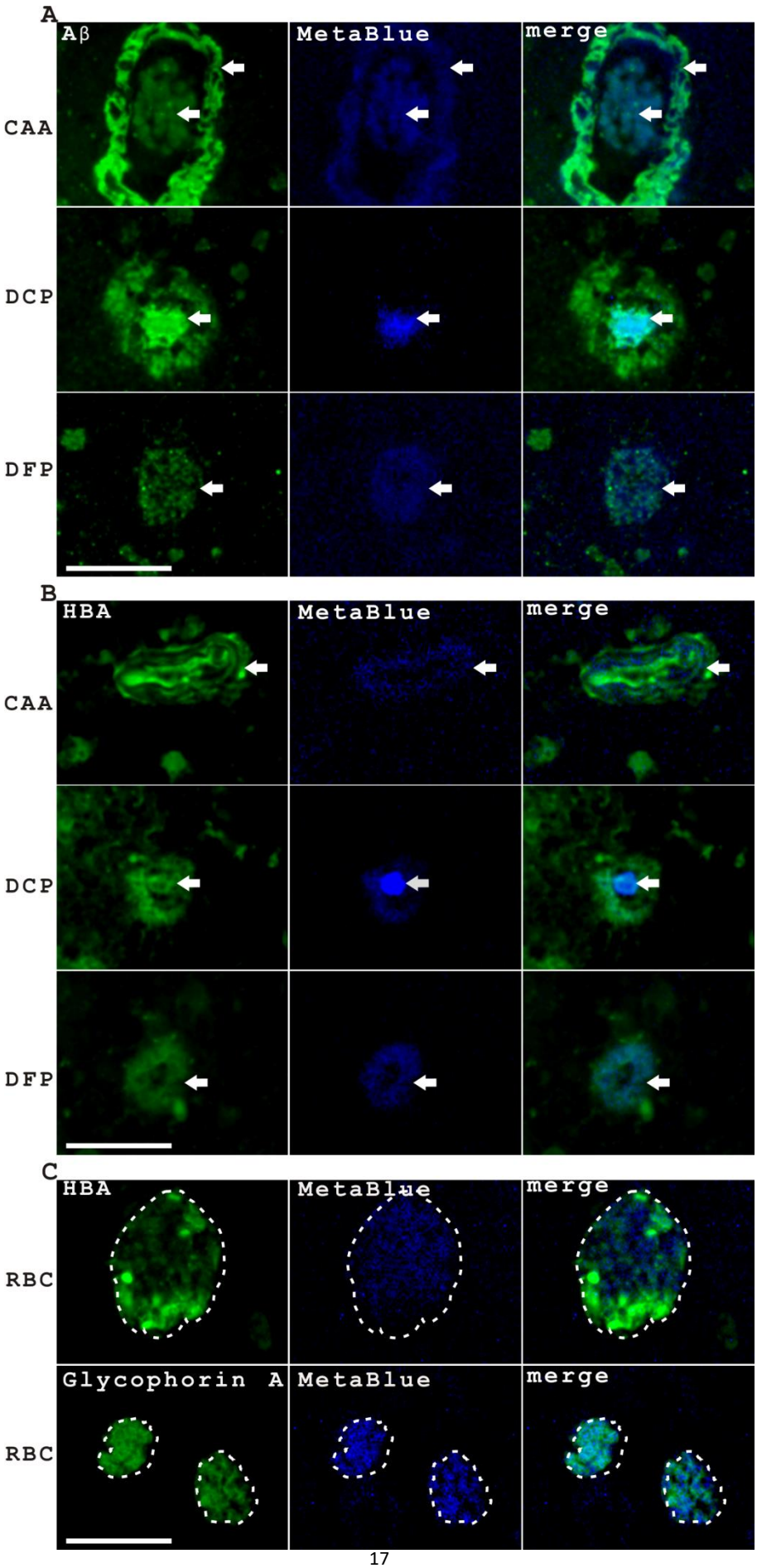

331

Figure 4. The MetaBlue blue autofluorescence signals overlapped with Aβ and alpha hemoglobin (HBA) staining in CAA, dense-core plaques and diffusive plaques and were also present in the red blood cells. A. MetaBlue signals co-stained with Aβ in CAA, dense-core plaques (DCP) and diffusive plaques (DFP). **B.** MetaBlue signals co-stained with HBA staining in CAA, dense-core plaques, and diffusive plaques. **C.** MetaBlue signals were clearly observed in red blood cells (RBC) labeled either with HBA or with Glycophorin A. The arrows pointed to the co-expression of markers. Dashed lines indicated red blood cell clusters with overlapping MetaBlue staining. Scale bar, 50 μm.

The association of blood markers HBA, HbA1c, ApoE, CD42b with senile plaques

To directly check the association of Aβ with blood markers， we did co-staining of Aβ with red blood cell marker HBA and HbA1C (shown in Figure 5), blood plasma marker ApoE and platelet marker CD42b (shown in Figure 6). Aβ staining was observed to associate with HBA staining in CAA, in dense-core plaques and in diffusive plaques (Figure 5A). However, not all senile plaques showed the same intensity HBA staining. In some diffusive plaques, HBA immunostaining signals were very weak (Figure 5A, bottom). The heterogeneity of HBA signals in senile plaques likely reflected the heterogeneous and dynamic nature of senile plaque formation, which was repeatedly observed in our experiments with multiple markers. More pictures showed the red blood cell Aβ staining was provided in Supplementary Figure 2. Since HbA1C is a glycation product of hemoglobin, which is also related to diabetes and aging changes of red blood cells[24], we decided to check the expression of HbA1C in senile plaques. The experiment results indicated that HbA1C staining also associated with Aβ staining in CAA, in dense-core plaques and in diffusive plaques (Figure 5B).

Since ApoE is a plasma protein that associates with Aβ, which is an important modifier of AD risk[25], it is important to examine the interactions between Aβ and ApoE during senile plaque development. We observed that Aβ staining associated with ApoE in small

or large patches in the blood vessel lumens, and also in CAA and perivascular plaques, in dense-core senile plaques and in diffusive senile plaques (Figure 6A). The frequent presence of ApoE in blood vessel lumen suggested that ApoE is mostly derived from the blood (Figure 6A, second and third panels). In addition, ApoE intensity was highly variable in senile plaques while senile plaque Aβ intensity is relatively stable, which again suggested the dynamic nature of senile plaques (Figure 6A, bottom two panels). ApoE associated with senile plaques of different morphologies such as dense-core or diffusive senile plaques and with different sizes regardless they were large or small, with more pictures shown in Supplementary Figure 3. We think that ApoE could be an additional constitutive component of senile plaques besides Aβ and MetaBlue.

Platelets are another important type of cells in the blood that frequently link to blood abnormalities in many diseases. Platelets was previously thought to be related to senile plaque formation and be an important source of AβPP[26]. We used CD42b as a marker of platelets to analyze the behavior of platelets during senile plaque formation. We found that Aβ-positive and CD42b-positive platelets attached to blood vessel walls, indicating the presence of blood vessel damage as it is well-known that blood vessel wall damage activates platelets and attracts platelets to the damage sites (Figure 6B, top). Large aggregations of CD42b-positive platelets with clearly detectable Aβ expression were also found in the blood vessels, suggesting the happening of intravascular coagulation (Figure 6B, middle). Additionally, CD42b-positive platelets were found in dense-core senile plaques (Figure 6B, bottom). However, the staining intensity of Aβ on platelets was in general lower comparing to what we observed in Aβ-positive red blood cells in AD brain tissues. With complicated regulations between platelets and red blood cells[27-30], platelet could be another significant player involving blood leakage and senile plaque formation.

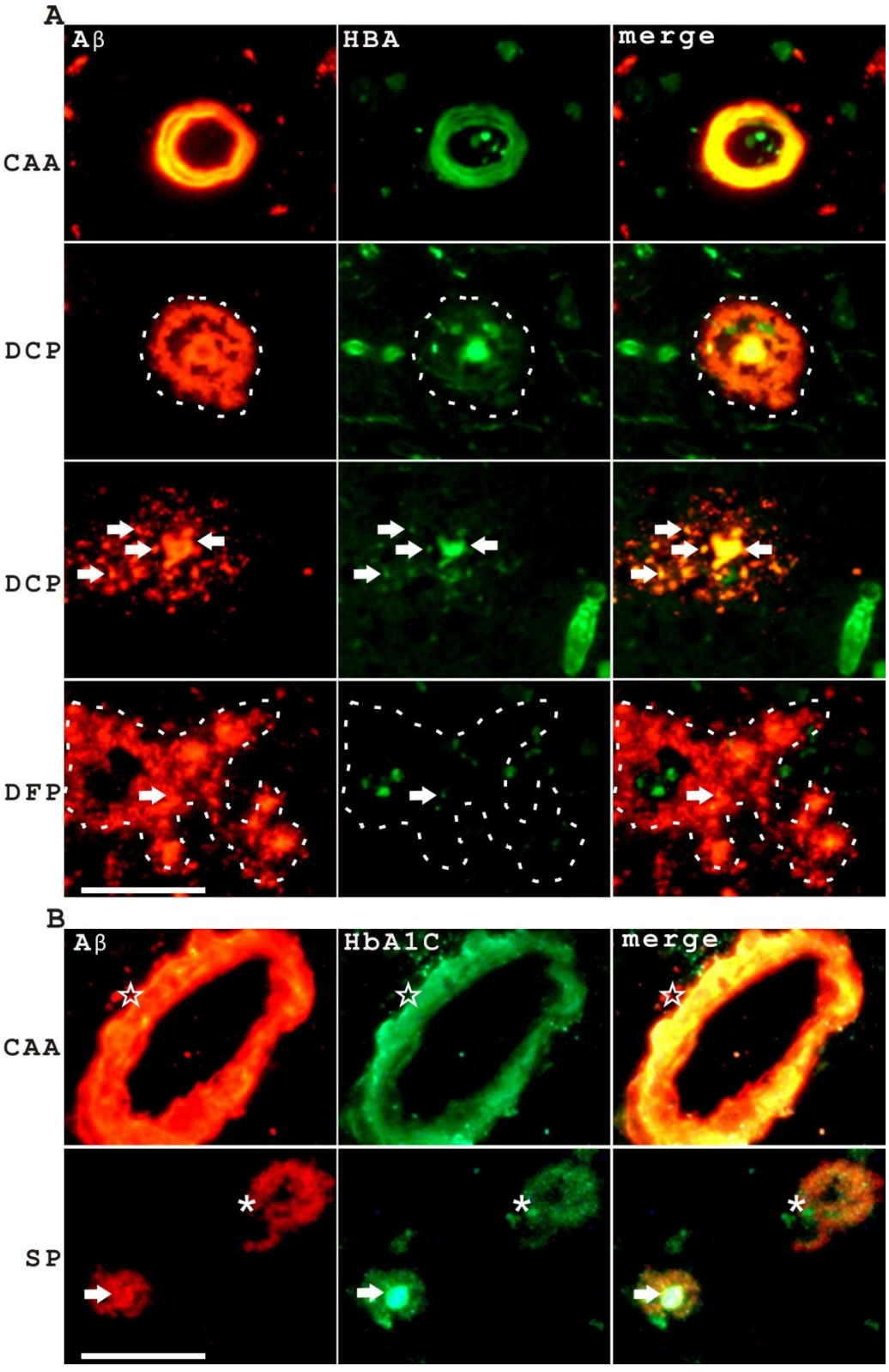

Figure 5. Hemoglobin colocalized with Aβ during different stages of senile plaque development. A. Red cell markers HBA co-expressed with Aβ at different stages of senile plaque development, in CAA, dense-core plaques and diffusive plaques. However, not all senile plaques display strong HBA staining. Some large diffusive

394 plaques with very weak HBA staining were also observed (bottom). The dashed lines
395 indicated dense-core senile plaques or diffusive plaques. The arrows indicated some
396 diffusive Aβ aggregates. **B.** Red cell marker HbA1C (glycated hemoglobin） also co-
397 expressed with Aβ in CAA (indicated with pentagons) and dense-core plaques
398 (indicated with arrows) and diffusive plaques (indicated with asterisks). Scale bars, 50
399 μm.
400
401

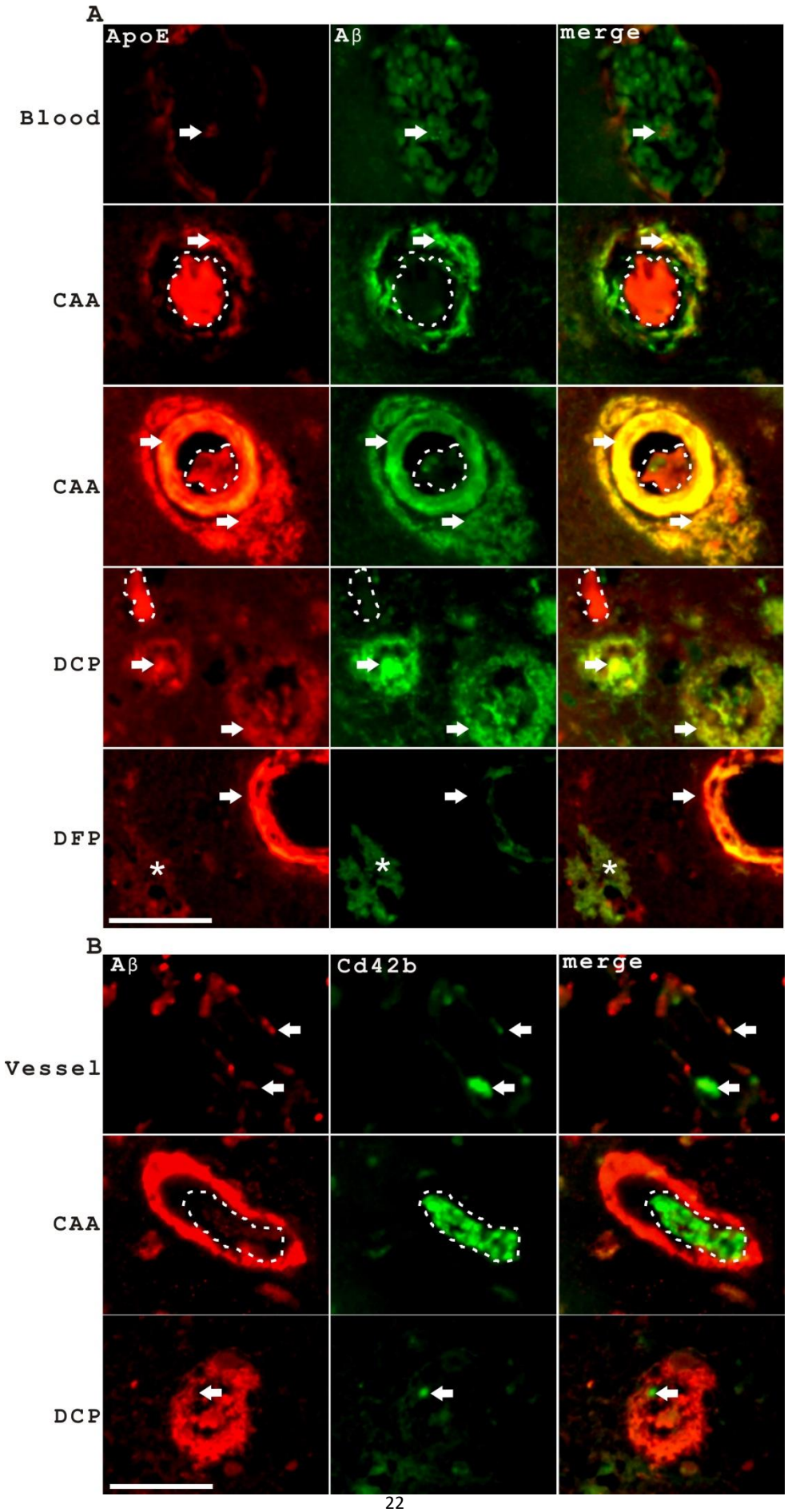

402

Figure 6. The association of blood marker ApoE and platelet marker CD42b with senile plaque development. A. ApoE associated with Aβ in small blood cell patches in the vessel (top), in large patches in the vessel and in perivascular plaques (second panel), in CAA (third panel), in dense-core senile plaques (fourth panel) and in diffusive plaques (bottom). Arrows indicated the co-expression of markers in CAA and senile plaques. Dashed lines indicated the staining in luminal blood patches. The asterisk indicated a diffusive senile plaque with ApoE staining much weaker than neighboring CAA. **B.** CD42b-labeled platelets participated senile plaque development. Platelets with Aβ expression were observed in platelets adhering to vascular wall (top) or in platelet aggregations in the blood vessel (middle). Platelets were also observed directly in senile plaques (bottom). The arrows indicated the platelets. The dashed lines indicated a patch of aggregated platelets. Scale bars, 50 μm.

The dynamic interaction of Aβ expression and vascular degeneration during senile plaque development examined with ColIV, ACTA2 and LRP1 staining

CAA, vascular degeneration and microhemorrhage have been long implicated to be involved in the senile plaque formation[9,10,12,17,18]. However, the exact contribution of blood vessels to senile plaques is not so clear. We used ColIV as a blood vessel marker to examine the blood vessel changes during the senile plaque formation process (Figure 7). As it is well-known, ColIV labels the extracellular matrix collagen component of the blood vessels. Firstly, we observed patches of strong Aβ staining with diffusive luminal ColIV staining in the blood vessels, an indication of blood vessel damage (Figure 7, top). We also observed Aβ staining associates with ColIV staining in vessel walls in CAA (Figure 7, second panel). In CAA blood vessels, some overlapping of Aβ and ColIV staining was observed, suggesting Aβ probably was accumulated in the vessel extracellular matrix. In addition, we observed strong perivascular Aβ staining with concurrent diffusive ColIV staining, again indicating blood vessel damage (Figure 7, third panel). Moreover, balloon-shape bulge formation in large blood vessels was also detected (Figure 7, fourth panel). These bulges contained condensed staining of Aβ

433 that was surrounded by degenerative ColIV staining, indicating that blood vessel
434 aneurysm could be formed, which might be a way to induce dense-core senile plaques.
435 This observation is consistent with a previous study stating lumpy and bumpy blood
436 vessels were found in AD brain tissues by using scanning electron microscopy[31]. The
437 tight association between senile plaque formation and vascular degeneration was
438 observed in both dense-core senile plaques (Figure 7, fifth to seventh panel) and
439 diffusive senile plaques（Figure 7, bottom). Our observation suggested that the senile
440 plaque formation is intrinsically linked with vascular degeneration and
441 microhemorrhage with blood-borne Aβ leakage.
442
443

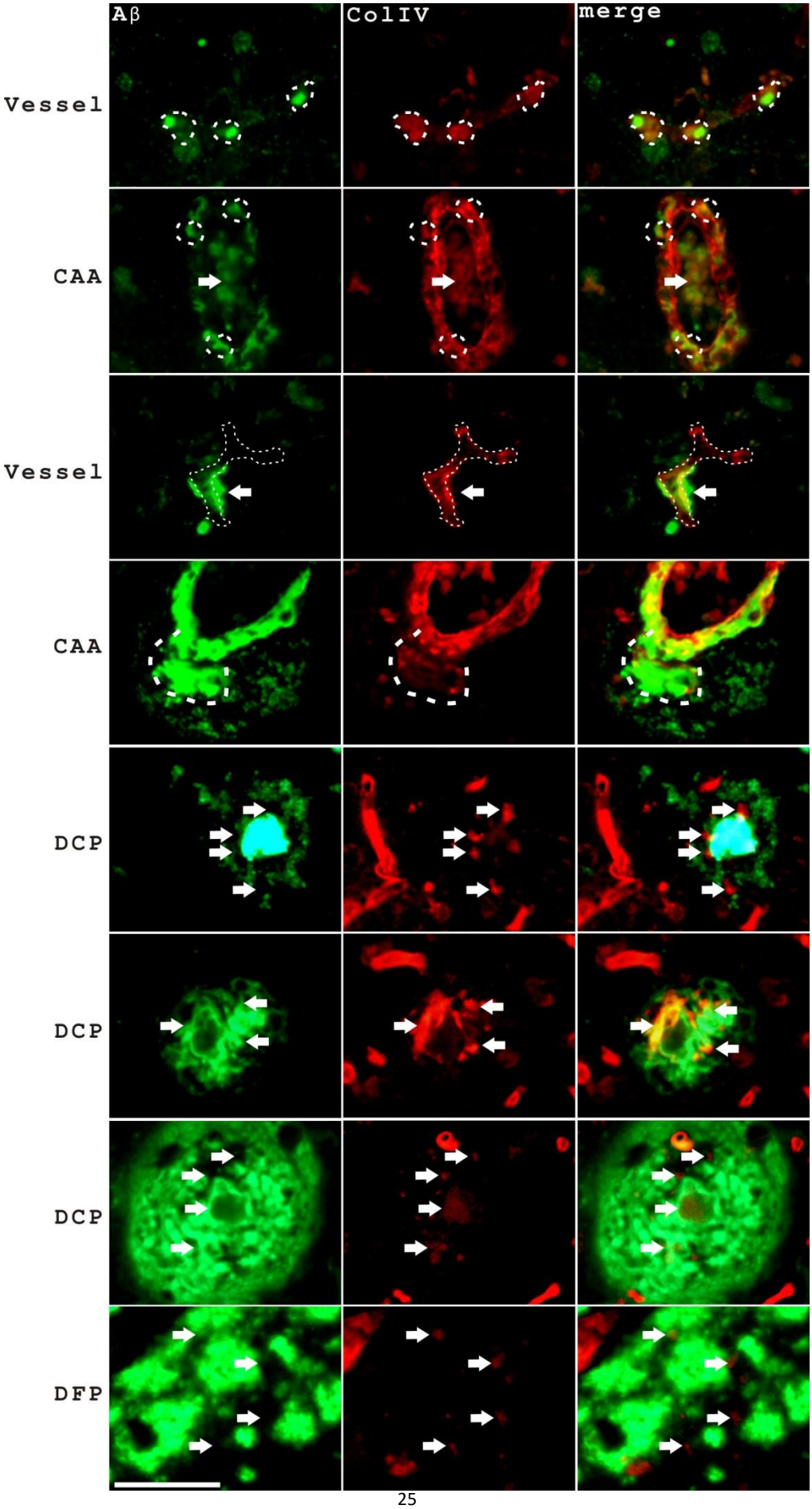

444

Figure 7. The dynamic interaction of Aβ expression and blood vessel alterations in senile plaque development. Discrete condensed Aβ staining was observed in a blood vessel accompanying diffusive ColIV staining in the vessel lumen (indicated by dashed lines in the top panel). Aβ staining associated with CAA blood vessel wall (indicated by dashed circles) and also blood cells (indicated with arrows in the second panel). Aβ perivascular staining (indicated with arrows in the third panel) was associated with a "dissolving" blood vessel phenotype (indicated with dashed lines) with diffusive ColIV staining in the vessel lumen. A bulge-like structure (indicated with dashed lines in the fourth panel) was observed in a large blood vessel containing concentrated Aβ, suggesting blood vessel aneurysm might be happening. Three examples of dense-core senile plaques showed degenerated blood vessel remnants (indicated with arrows in the fifth, sixth, seventh panels) scattering around senile plaque structures. An example of a diffusive senile plaque intermingled with degenerated vessel remnants (indicated with arrows in the bottom panel) was also shown. Scale bar, 50 μm.

To further illustrate the relationship of vascular defects with senile plaque formation, we also analyzed two other blood vessel related markers ACTA2 and LRP1. ACTA2 labels the smooth muscle cells of the blood vessels. LRP1 is an ApoE receptor involving Aβ clearance that expresses strongly in the endothelium of blood vessels[32,33]. Our experiment showed that in early stages of CAA development, ACTA2 staining regions were mostly complementary to Aβ staining regions in the blood vessels, suggesting that the initial Aβ in the CAA blood vessel probably resided in the blood vessel extracellular space (Figure 8A, top). This is consistent with the observations of some overlapped staining between Aβ and ColIV, which is a marker of blood vessel extracellular matrix. These observations hinted that CAA is probably formed by blood leakage through the endothelial cell barrier into blood vessel extracellular matrix. We also observed diffusive staining of ACTA2 in CAA blood vessel lumen and some large diffusive patches of ACTA2 staining in the AD brain tissues (Figure 8A, second and third panels), both of which indicated blood vessel degeneration, similarly as it was shown by diffusive ColIV staining. Additionally, degenerated blood vessel remnants marked with

ACTA2 were also observed in the center of senile plaques (Figure 8A, bottom), further confirming the direct relation between senile plaque formation and vascular degeneration.

LRP1 was observed to label the blood vessels with diffusive luminal staining of Aβ (Figure 8B, top). LRP1 also clearly labeled blood vessel structures surrounding the center of dense-core senile plaques (Figure 8B, middle and bottom). We also observed that condensed Aβ came out of blood vessels precisely on site through openings on the vessel wall (indicated with arrows in Figure 8B, middle and bottom panels). Small vessel degeneration with Aβ in the lumen might be another way to produce dense-core plaques besides blood vessel aneurysm.

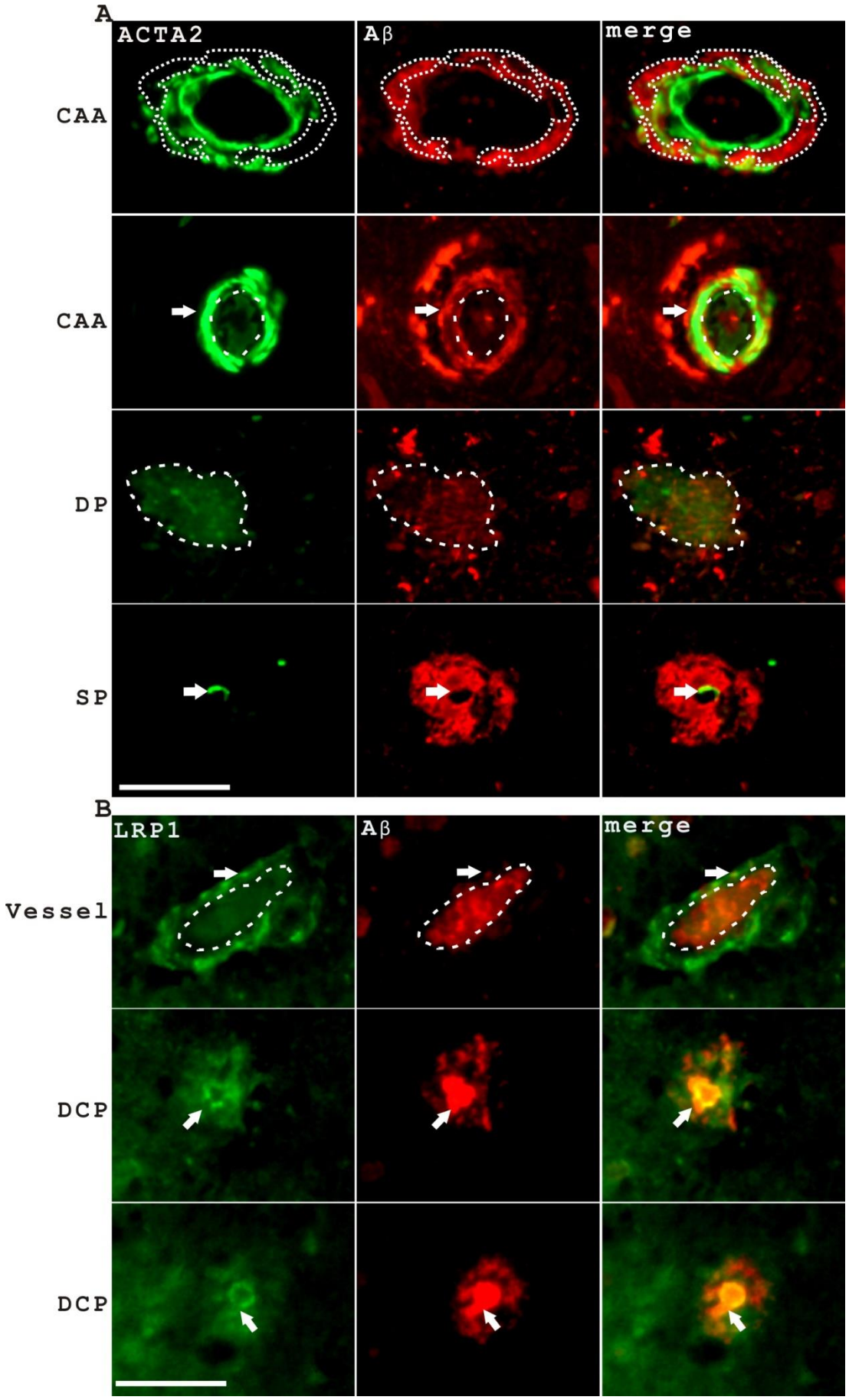

487

Figure 8. The dynamic interaction of Aβ expression and blood vessel marker ACTA2 and LRP1 in senile plaque development. A. The dynamic interaction of Aβ expression and blood vessel marker ACTA2 in senile plaque development. CAA Aβ staining mostly showed a complementary expression pattern relative to ACTA2, a smooth muscle cell marker (indicated with dashed lines in the top panel). ACTA2 staining was also observed in the vessel lumen (indicated with dashed lines in the second panel) of a CAA blood vessel (indicated with an arrow). A diffusive patch (DP) of ACTA2 staining, an indication of blood vessel degeneration, was observed to associate with diffusive, fibrillar Aβ staining (indicated with dashed lines in the third panel). Degenerated blood vessel remnants with ACTA2 staining were also observed in the center of a senile plaque (indicated with arrows in the bottom panel). **B.** The dynamic interaction of Aβ expression and blood vessel marker LRP1 in senile plaque development. LRP1 expression was observed in the blood vessel wall, also in the blood vessel structures in the dense-core senile plaques (DCP). The arrows indicated the co-expression of markers. Scale bar, 50 μm.

Blood vessel Aβ expression associates with red blood cell damage and vascular damage

After repeated experiments of Aβ staining in the blood cells and in the blood vessels, it came clear to us that Aβ does not distribute evenly among blood cells or along the blood vessels. It appeared that Aβ was associated with patches of red cells with reduced and diffusive HBA staining, an indication of red blood cell damage or hemolysis (Figure 9A, top three panels). Sometimes, specific ring-shape Aβ stained structures were observed in the blood vessels, which associated with red blood cells (Figure 9A, bottom). Aβ staining was stronger in blood vessels with diffusive ColIV staining in the vessel lumens (Figure 9B, top), suggesting an Aβ association with the solubilization and damage of blood vessel structures. Some strongly stained Aβ aggregates began to emerge in the fields of diffusive Aβ staining associated with vascular degeneration with diffusive ColIV staining (Figure 9B, bottom two panels). Thus, the Aβ staining in the

518 blood vessels was closely associated with both red blood cell damage and vascular
519 damage.
520

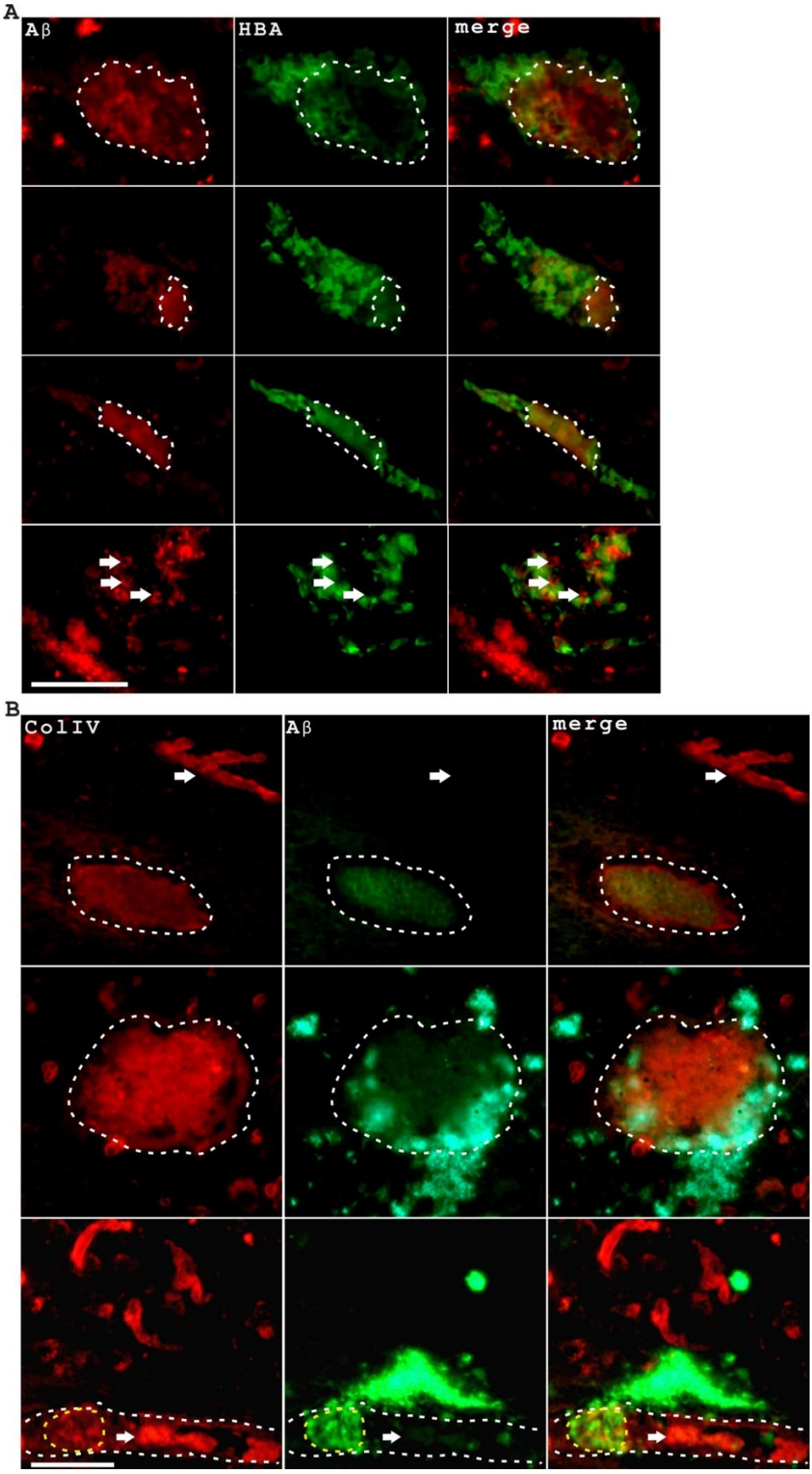

521

Figure 9. Aβ staining in the blood vessels associates with red cell damage and vascular damage. A. Aβ staining in the blood vessels associated with red cell damage. Top three panels showed images indicating the association of Aβ staining with weak and diffusive Hb staining, a sign of red blood cell damage or hemolysis. The bottom panel showed some ring-shape structures with Aβ staining formed closely around red blood cells. **B.** Aβ staining in the blood vessels associated with vessel damage. Aβ staining in a blood vessel with diffusive ColIV staining in the vessel lumen (marked with dashed lines) was compared to a normal looking vessel with clear ColIV vessel outline staining (marked with an arrow in the top panel). A large area of diffusive ColIV and Aβ staining with degenerating vessel walls was observed (marked with dashed lines in the middle panel). Some Aβ aggregations with bright staining also formed within this area. The bottom panel indicated a vessel with collapsed ColIV-positive components in the vessel lumen that intermingled with a strong Aβ staining. Some areas of strong luminal ColIV staining but with weak Aβ staining were also observed. The dashed lines indicated the blood vessel or the diffusive luminal ColIV-positive areas. Scale bar, 50 μm.

Aβ staining in the blood vessels and the in senile plaques is associated with Cathepsin D expression

The enhancement of Aβ staining in damaged red blood cells or in the vascular domains with vascular damage could be due to either enhanced expression of Aβ-related peptides or enhanced aggregation of Aβ monomers. Aβ aggregation is depending on both the synthesis of Aβ-related peptides and also the amyloidgenic activity of beta-site cutting enzymes. It is well known that hemolysis or vascular damage can activate platelets, which are able to secrete a large amount of AβPP. As for the beta-site cutting enzymes，besides BACE1, the assumed main beta-site cutting enzyme[34,35], with ongoing debates, many other proteases also have potential beta-site cutting activity, such as Cathepsin D[36-38], Cathepsin B[39,40], Carboxypeptidase B[41] and MMP2[42]. Cathepsin D was associated with AD risk genetically[43,44] and was also found to be present in senile plaques by

552 previous researches[45,46]. In our previous study investigating the relation between
553 lysosomal Cathepsin D and senile plaque development, we unexpectedly found that
554 domains of enhanced Aβ staining in the blood vessels coincided with luminal Cathepsin
555 D expression (Figure 10A, top). Some small but strongly stained Aβ aggregates
556 emerged in the luminal domains with diffusive Cathepsin D expression (Figure 10A,
557 second panel). Additionally, in CAA blood vessels, there existed patches of strong
558 Cathepsin D expression associating with significant Aβ staining (Figure 10A, third
559 panel). It was also clear that CAA blood vessel walls were Cathepsin D-positive. The
560 connection between Cathepsin D and Aβ expression was further strengthened when we
561 extended the investigation into senile plaques (Figure 10B). Very surprisingly, with
562 optimized immunostaining conditions，we observed that senile plaques came with a
563 constitutive Cathepsin D expression. Apparently, in senile plaques, there were two
564 distinct layers of Cathepsin D staining. One layer was a strong, granule type of
565 Cathepsin D staining, typical of lysosomes, which stained complementary locations
566 related to Aβ staining in senile plaques (Figure 10B, first, third and fifth panels).
567 Another type was a weaker and diffusive Cathepsin D expression, which often stained
568 a large portion of senile plaque area and showed overlapping staining with Aβ (Figure
569 10B, second, fourth and sixth panels). This constitutive Cathepsin D staining was often
570 detected in dense-core senile plaques. In diffusive senile plaques, the constitutive
571 Cathepsin D expression was weak, however, still detectable. The heterogeneity of
572 constitutive Cathepsin D intensities in senile plaques is probably due to the dynamic
573 nature of senile plaques, especially because they are self-digestive compartments highly
574 enriched for proteases such as Cathepsin D. The two-layer Cathepsin D expression
575 pattern in the senile plaque was further confirmed with a different Aβ/Cathepsin D
576 primary antibody pair, with similar results shown in Supplementary Figure 4.
577
578 We suspected that the constitutive Cathepsin D expression was coming from hemolysis
579 and vascular degeneration so that we co-stained Cathepsin D with red blood cell
580 markers (Figure 11). Cathepsin D expression in the blood vessels correlated with
581 domains of diffusive and reduced HBA staining, an indication of red cell damage

582 (Figure 11A, top panel). Cathepsin D expression also associated with HBA staining in
583 CAA and dense-core plaques, which additionally overlapped with plaque MetaBlue
584 staining (Figure 11A, bottom two panels). Another red blood cell marker HbA1C also
585 associated with Cathepsin D expression in CAA blood vessels, in diffusive MetaBlue
586 positive areas, and in dense-core senile plaques with strong MetaBlue signals (Figure
587 11B). These staining results suggested that the constitutive Cathepsin D in senile
588 plaques likely derived from hemolysis.
589
590

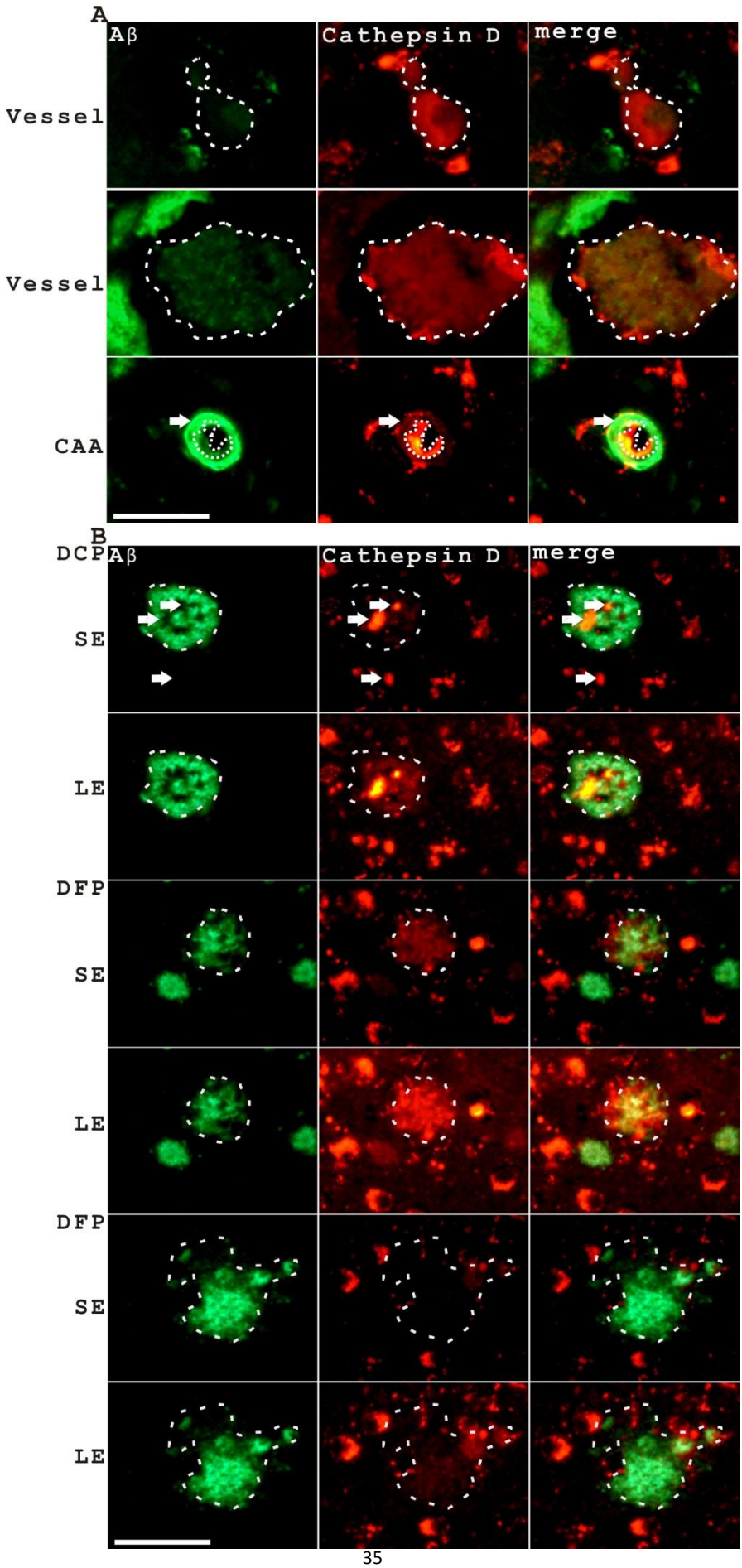

591

Figure 10. The association of Aβ and Cathepsin D in blood vessels and in senile plaques. A. Diffusive Aβ staining associated with diffusive Cathepsin D staining in the blood vessels. Diffusive Aβ staining co-distributed with diffusive Cathepsin D staining in non-CAA type of blood vessel lumen (top two panels). Aβ staining also associated with Cathepsin D staining in the lumen of a CAA blood vessel (bottom panel). Cathepsin D staining on the CAA vessel wall was also observed. Dashed lines indicated vessel diffusive Cathepsin D and Aβ staining. The arrow indicated a CAA blood vessel. **B.** Senile plaques overlapped with a constitutive but relatively weak Cathepsin D expression. A dense-core senile plaque (top two panels, DCP) had two distinct pattern of Cathepsin D staining. A strong and granule-like Cathepsin D staining showed at complementary positions relative to Aβ staining with the Cathepsin D image taken at a short exposure of 0.5 second (SE stands for short exposure) while the exposure setting for Aβ staining was not changed. A weaker and diffusive Cathepsin D staining co-distributed with Aβ staining in the senile plaques was also observed with the Cathepsin D image taken at a longer exposure of 1 second (LE stands for long exposure). The exposure setting of Aβ images was unchanged. A diffusive plaque (middle two panels, DFP) also showed a constitutive Cathepsin D staining that co-distributed with Aβ staining but not totally matching the outline of the senile plaque. A large diffusive plaque (bottom two panels, DFP) with less detectable constitutive Cathepsin D staining. Dashed lines indicated the regions of senile plaques. The arrows indicated strong and granule-like Cathepsin D staining. Scale bar, 50 μm.

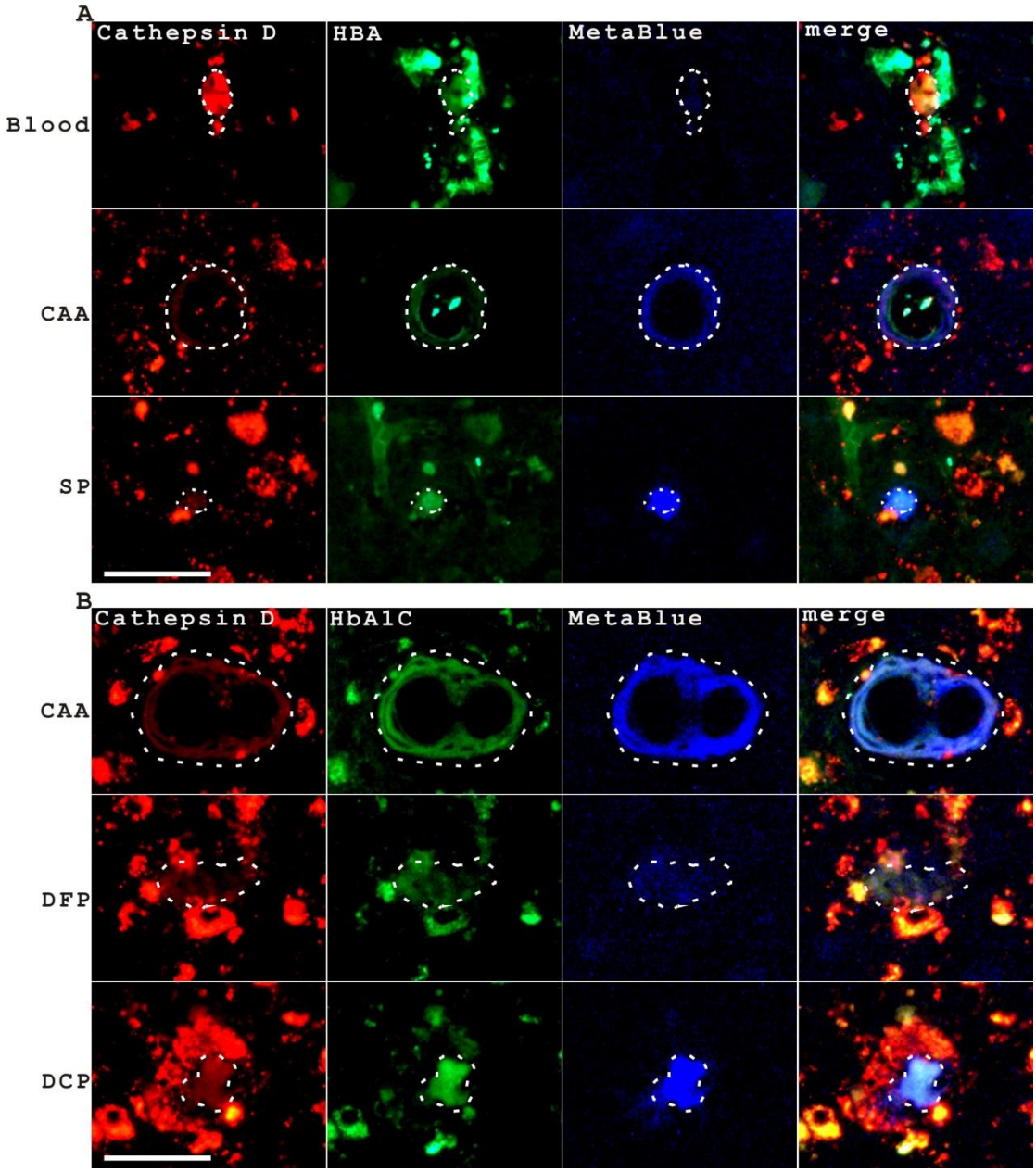

Figure 11. The association of Cathepsin D and hemoglobin in CAA and in senile plaques. A. Cathepsin D staining associated with HBA staining in the blood vessels, CAA and senile plaques. Cathepsin D staining associated with reduced RBC HBA staining (indicated with dashed lines in the top panel). Cathepsin D staining also associated with HBA staining in a CAA blood vessel with concurrent MetaBlue staining (indicated with dashed lines in the middle panel). In the bottom panel, a senile plaque (SP) (marked with dashed lines) showed both Cathepsin D and HBA staining with also a strong MetaBlue staining. **B.** Cathepsin D staining associated with HbA1c staining in

CAA, diffusive patches and senile plaques. Cathepsin D staining associated with HbA1C staining in a CAA blood vessel (top panel). A region of diffusive Cathepsin D staining also co-expressed diffusive HbA1C staining and MetaBlue staining was shown in the middle panel. A dense-core senile plaque structure with both Cathepsin D and HbA1C staining and also strong MetaBlue signals were shown at the bottom panel. Dashed lines indicated the selected regions of Cathepsin D and HbA1C co-expression. Scale bar, 50 μm.

The specific association of Cathepsin D and ApoE with Aβ in hemolysis in AD brain tissues.

Since accumulating evidence pointed out the importance of hemolysis during senile plaque formation, we did a more focused experiment investigating hemolysis in AD tissues. In a previous investigation regarding the relation between copper ions and senile plaque formation, we unexpectedly found that a copper iron staining dye named Rhodanine could be a good histological staining reagent of red blood cells and hemolysis as shown in Figure 12. Using this dye, we observed that there was widespread intravascular hemolysis or extravascular hemolysis in AD tissues. This dye also labels CAA blood vessels, confirming the relation between CAA and hemolysis (Figure 12A). Rhodanine staining associated with the whole spectrum of Aβ staining patterns related to senile plaque formation, from initially very weak expression in phenotypically normal red blood cells to enhanced Aβ staining in hemolysis, to strong staining in CAA and senile plaques (Figure 12B). In diffusive senile plaques, Rhodanine staining was very weak, suggesting that Rhodanine-positive substances might be metabolized after hemolysis during the course of senile plaque development (Figure 12B, bottom).

With Rhodanine staining as a tool to detect hemolysis, we analyzed the interaction between Aβ with Cathepsin D or ApoE during hemolytic events (Figure 13). The experiment results indicated a tight coupling of the Cathepsin D-Aβ association or

ApoE-Aβ association with hemolysis, regardless the hemolysis happened intravascularly or extravascularly. Aβ staining in hemolysis was usually weaker than mature senile plaques (Figure 13A, top two panels and Figure 13B, top two panels). However, we frequently observed some strongly-stained Aβ aggregates began to form from the weakly-stained Aβ-positive hemolytic areas with overlapping Cathepsin D or ApoE staining (Figure 13A, bottom panel and Figure 13B, bottom panel). These results suggested that hemolytic domains might be the initial seeding and fermenting grounds of amyloid aggregate formation. To our knowledge, this is the first time that a transitional stage for senile plaque formation has been defined.

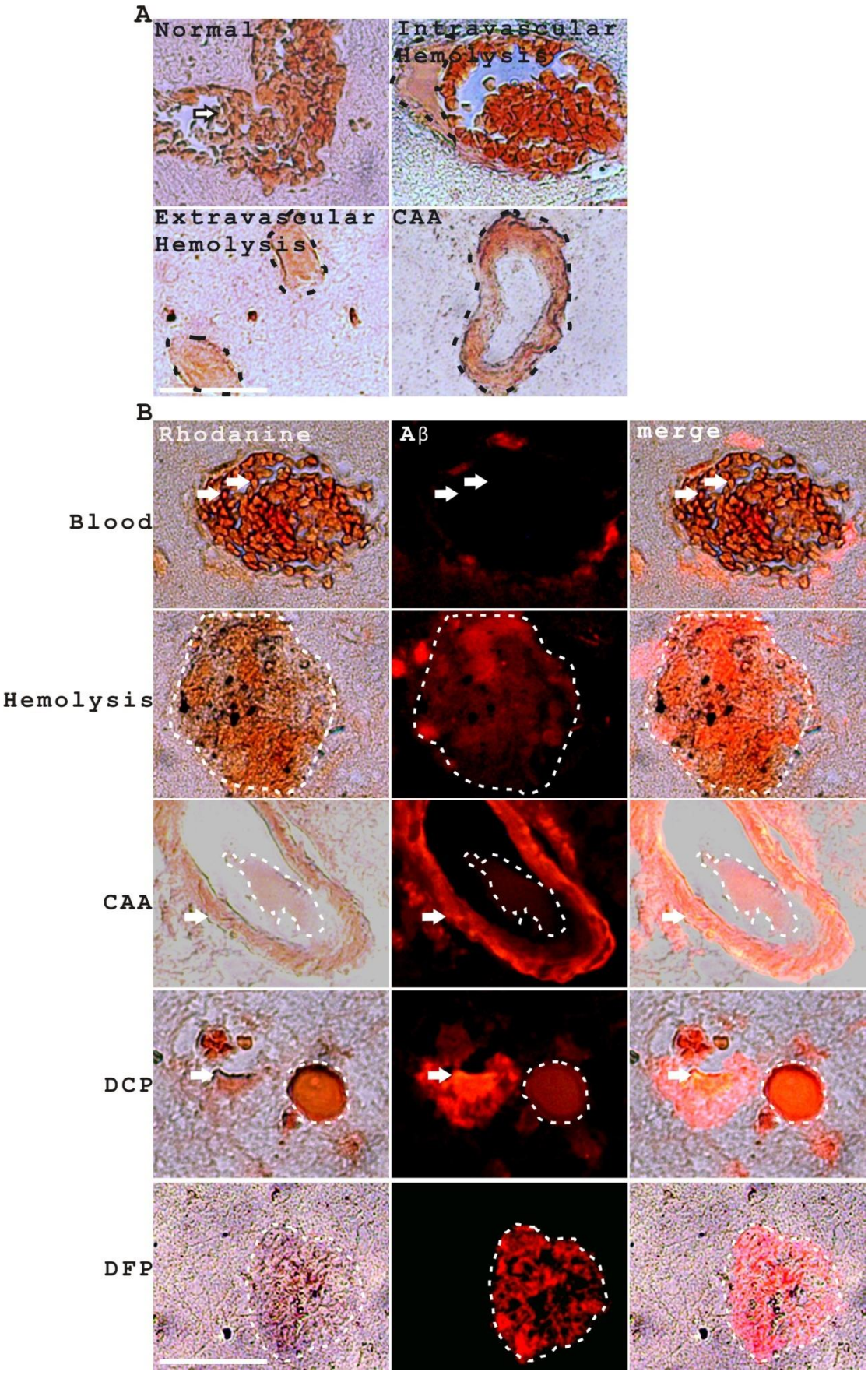

668 **Figure 12. Rhodanine staining showed widespread hemolysis in AD brain tissues.**
669 **A.** Rhodanine staining was a good marker of normal red blood cells, which also stained
670 hemolysis, and CAA in AD brain tissues. **B.** Rhodanine staining was present in
671 normally looking red blood cells without strong Aβ staining and at all different stages
672 of senile plaque development including hemolysis, CAA with hemolysis, dense-core
673 plaques (DCP) and diffusive plaques (DFP) with enhanced Aβ staining. Scale bar, 50
674 μm.
675
676

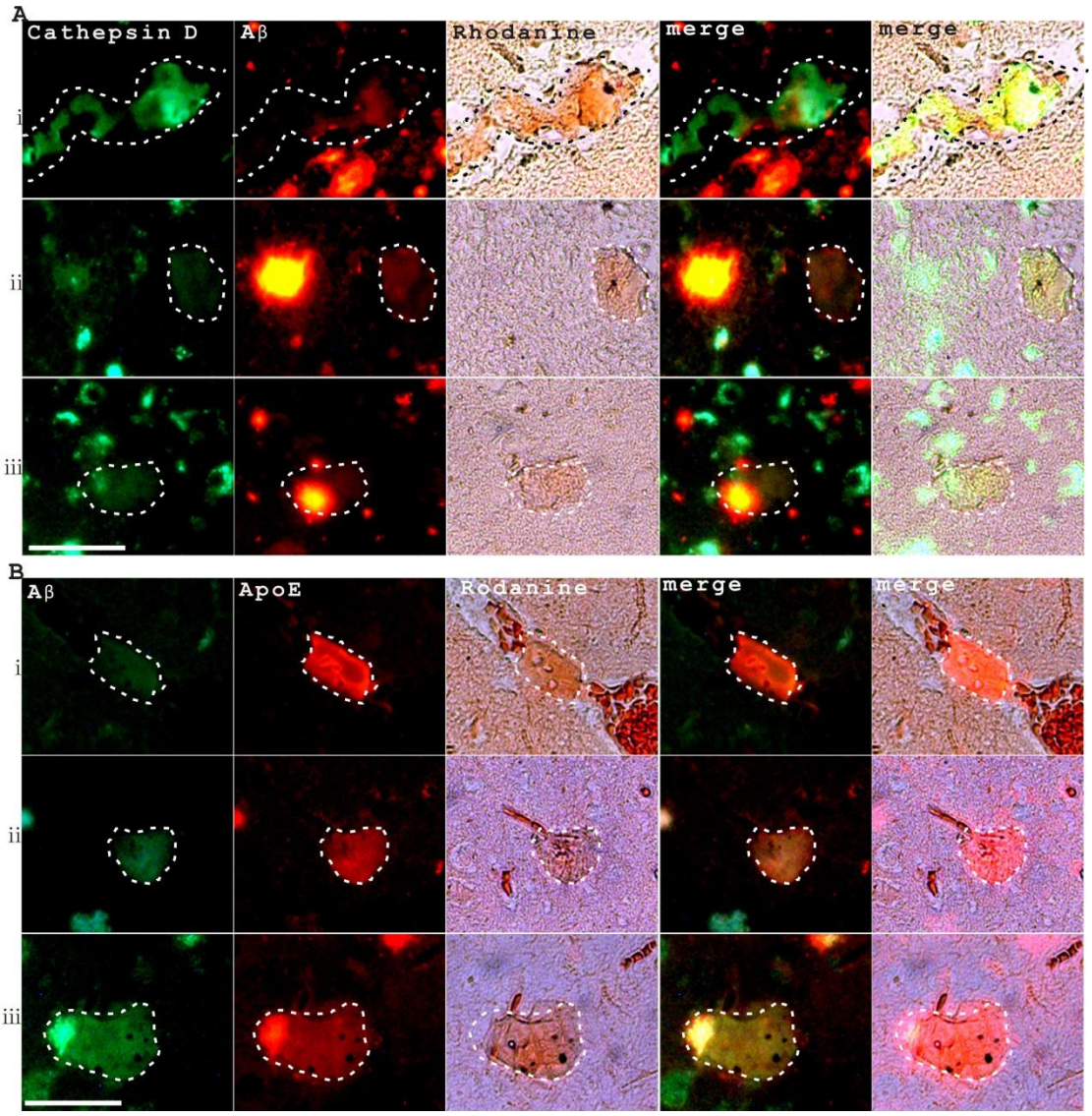

677
678 **Figure 13. Cathepsin D and ApoE both associated with Aβ specifically in hemolysis.**
679 **A.** Cathepsin D associated with Aβ in intravascular hemolysis (i) and extravascular
680 hemolysis (ii , iii). Some strong Aβ staining was observed in (iii). **B.** ApoE associated

with Aβ specifically in intravascular hemolysis (i) and in extravascular hemolysis (ii , iii). Some strong Aβ staining was observed in (iii). Scale bar, 50 μm.

Aβ forms protease-sensitive heterooligomer rapidly with hemoglobin while Aβ self-oligomers are protease-resistant.

Since the senile plaque formation process might start from hemolysis, we thought the initial Aβ aggregation might also have something to do with hemolysis. We hypothesized that HBA physically interacts with Aβ during hemolytic events. The potential interaction between hemoglobin and Aβ has been studied in the past in a few published studies[47,48], but the investigations were still not complete and comprehensive. We tested this hypothesis further with an aggreagation assay in the test tubes. First, we checked the self-oligomerization of Aβ peptides (Figure 14). Both Aβ40 and Aβ42 formed small aggregates immediately soon after dissolving the peptides in DMSO and diluted into PBS solution at 5 μM concerntration. Aβ40 formed aggregates with increasing size upon incubation up to 3 days, while the sizes of Aβ42 self-oligomer did not change significantly upon prolonged incubation (Figure 14A). Both Aβ 40 and Aβ42 aggregates were resistant to a 15-minute Proteinase K （PK） treatment, suggesting the self aggregates were protease-resistant (Figure 14B).

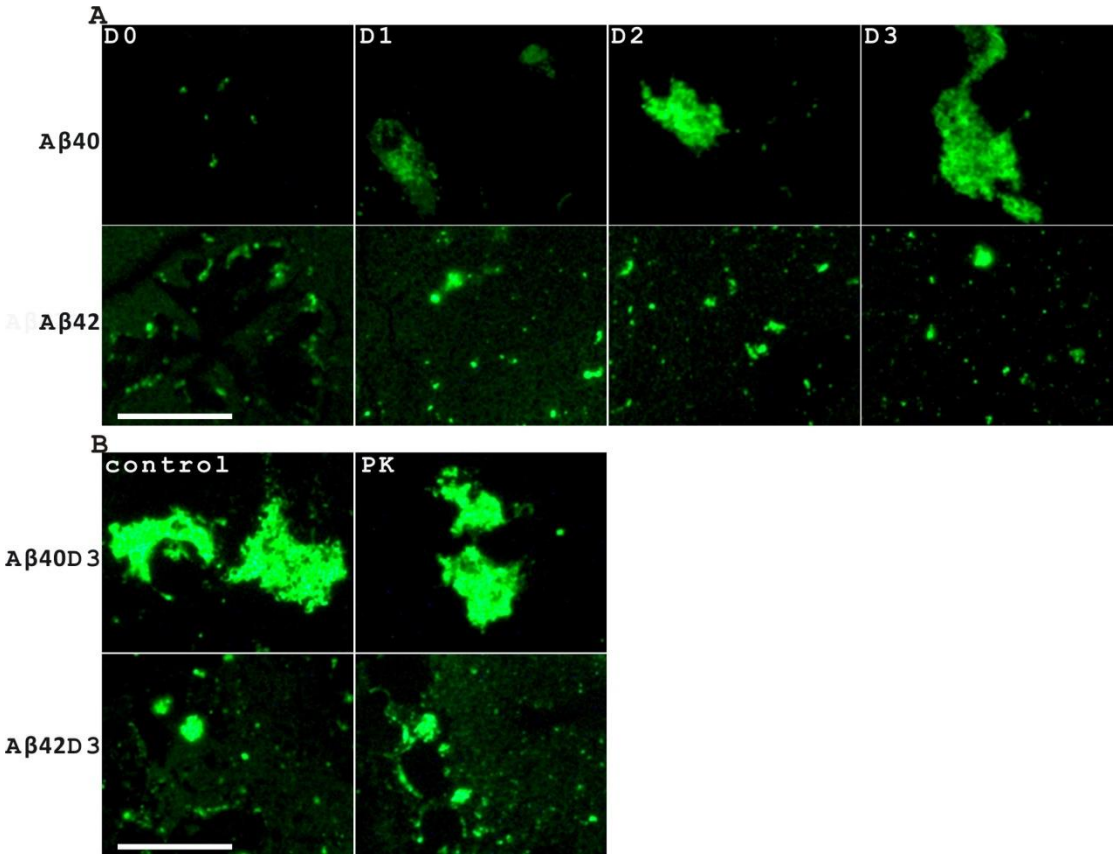

Figure 14. Aβ40 and Aβ42 form protease-resistant self-oligomers *in vitro*. A. Aβ40 and Aβ42 formed self-oligomers when incubating in PBS solution for up to 3 days (Day 0 to Day 3) followed with a drying up procedure by droplet evaporation. D0 stands for Day 0. **B.** Both Aβ40 and Aβ42 self-oligomers were resistant to Proteinase K (PK) treatment. Scale bar, 50 μm.

We then incubated hemoglobin and Aβ40 at a molar ratio of 1:4 (1.25 μM hemoglobin and 5 μM Aβ40), and checked the aggregation product out of this mixture. We observed that hemoglobin formed complexes with Aβ40 very quickly. Even in Day 0 samples, hemoglobin formed large leaf-like or ring-shape complexes with Aβ40 (Figure 15A, top two panels). Some dot-like structures dervied from Aβ40 self-oligomerization were also present in Day 0 samples (Figure 15A, third panel). Large leaf-like structures and ring-shape structures were continually present in Day 1, Day 2, Day 3 samples (Figure 15A, bottom four panels). In AD tissue samples, we did not observe large-leaf like structures with Aβ staining. However, we did observe some ring-shape structures with

718 overlapping staining of Aβ and hemoglobin (Figure 15B). This probably also explained
719 the ring-shape structures in Figure 9, which suggested that the ring-shape Aβ/Hb
720 complexes did form in the blood vessels of AD tissues *in vivo*.
721
722

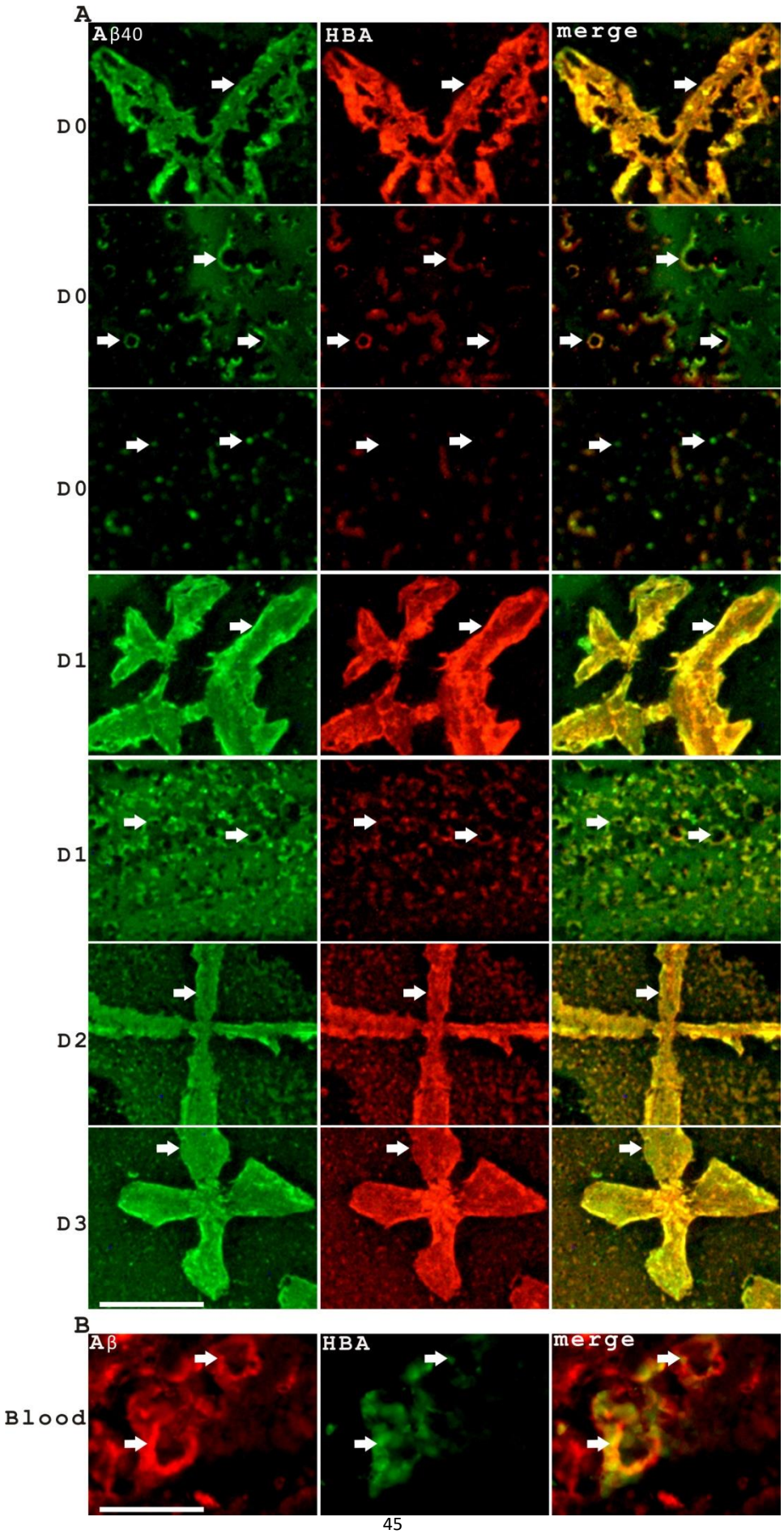

723

Figure 15. Aβ40 forms heterooligomer rapidly with hemoglobin. A. Aβ40 forms heterooligomer rapidly with hemoglobin when co-incubating in PBS solution for up to 3 days followed with sample drying by droplet evaporation. Co-immunostaining of Aβ and hemoglobin was shown for Day 0 (top 3 panels), Day 1 (fourth and fifth panels), Day 2 (the sixth panel) and Day 3 (the seventh panel) samples. Arrows indicated different structures, such as leaf-shape, ring-shape structures, that co-stained with both Aβ and HBA (alpha hemoglobin) antibodies. The dot shape structure likely represented Aβ40 self-oligomers. Special ring shape structures were indicated with arrows in the second and fifth panel. **B.** Aβ40 forms ring-shape structures interacting with hemoglobin in the lumens of AD patient blood vessels similar to the ring-shape structures formed in Aβ and hemoglobin mixture samples *in vitro*. Scale bars, 50 μm.

In Aβ42 and Hb mixed Day 0 samples, we observed leaf-shape, ring-shape, and line-shape structures with both Aβ42 and Hb staining (Figure 16). In Day 0 samples, we also see the existence of Aβ42 self-oligomers, which was less frequently detected in Day 1, Day 2 and Day 3 samples (Figure 16A), indicating that Aβ42/Hb interactions might compete out Aβ42 self-oligomerization. Previous studies suggested that hemin inhibits Aβ aggregation[49,50] and hemoglobin might interact with Aβ through the hemin motif[48], suggesting that a hemoglobin inhibition of Aβ self-oligomerization is likely. Large leaf-shape or smaller ring-shape structures were continually observed in Day 1, Day 2 and Day 3 samples (Figure 16, bottom three panels). Unlike the protease-resistant Aβ40 and Aβ42 self-oligomers, Aβ40/Hb and Aβ42/Hb hetero-complexes were both sensitive to PK treatment (Figure 16B).

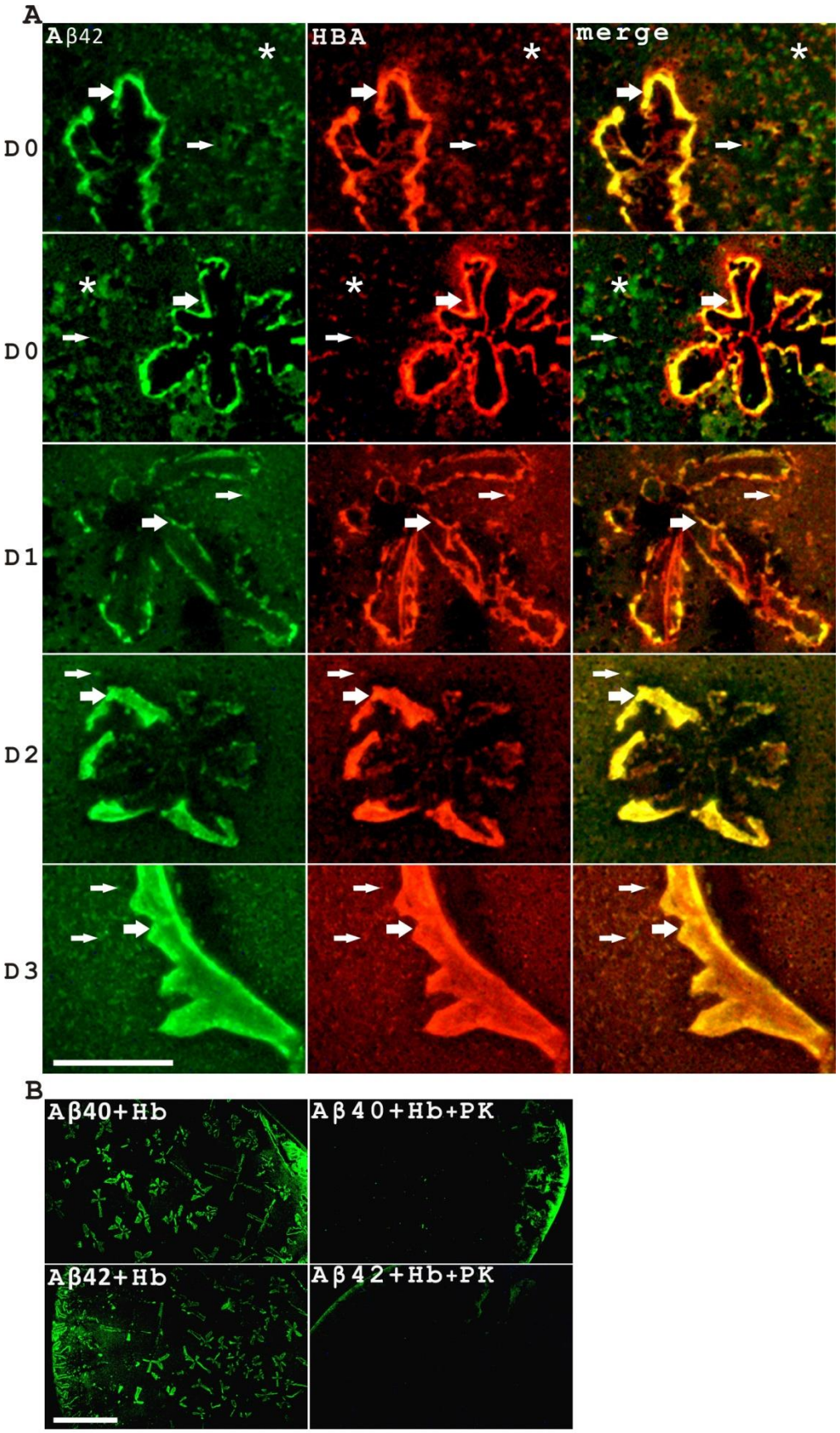

Figure 16. Aβ42 forms protease-sensitive heterooligomer rapidly with hemoglobin

752 **when co-incubating in PBS solution for up to 3 days followed with sample drying**
753 **by droplet evaporation. A.** Aβ42 forms heterooligomer rapidly with hemoglobin in
754 PBS solution. Co-immunostaining of Aβ and hemoglobin was shown for Day 0 (top
755 two panels), Day 1 (third panel), Day 2 (fourth panel) and Day 3 (fifth panel) samples.
756 Large arrows indicated relatively large structures while small arrows indicated smaller
757 structures. Leaf-shape, ring-shape or dot-shape structures were observed. Some self-
758 oligomers also existed in Day 0 samples, indicated with asterisks. Scale bar, 50 μm. **B.**
759 Both Aβ40/Hb and Aβ42/Hb complexes were protease-sensitive with the complexes
760 illustrated by Aβ antibody staining. PK treatment drastically decreased the signals of
761 resulting complexes. Scale bar, 200 μm.
762
763 **Discussion**
764
765 Senile plaque Aβ has been hypothesized to be derived from neural or vascular/blood
766 source[7,12,15,51]. This study indicated the primary direct source of Aβ is not neural cell
767 with the evidence showing a lack of substantial overlapping of senile plaque Aβ with
768 neural markers. Additionally, Aβ expression in neural cells appears to be too low to
769 account for the high density Aβ expression in senile plaques. Instead, senile plaque Aβ
770 most likely comes from red blood cell-associated Aβ leakage out of damaged blood
771 vessels. The evidence is the following: Firstly, red blood cells in AD patients were
772 clearly stained with Aβ antibody, especially in hemolytic red blood cells. Secondly,
773 strongly-stained Aβ aggregates emerged in the hemolytic regions thus hemolytic areas
774 were likely the initial seeding grounds of Aβ aggregation. Thirdly, senile plaque Aβ co-
775 distributed with multiple blood markers such as HBA, HbA1C, ApoE and red blood
776 cell-associated MetaBlue autofluorescence at multiple stages of senile plaque
777 development such as CAA, dense-core plaques and diffusive plaques.
778
779 Two important aspects of senile plaque formation are the source of Aβ peptides and the
780 source of beta-site cutting enzymes. This study indicated that hemolysis could be a
781 critical step that bring together Aβ-related peptides and Cathepsin D, a potential beta-

site cutting enzyme, which might help to initiate the Aβ aggregation process. Platelets could be an important source of Aβ-related peptides in the blood and in hemolysis. Our experiment indicated that CD42b-positive platelets are stained positive for Aβ in the blood vessel lumen and on the blood vessel walls. Since platelets can release AβPP in alpha-granules after platelet activation by hemolysis or vascular damage[26,52-54]，it is possible that some of Aβ that associated with red blood cells were actually derived from platelets. HBA, CD42b and Rhodanine staining indicated that both hemolysis and coagulation were present in AD blood vessels, suggesting that the disrupted blood homeostasis is a fundamental defect in AD patients. Cathepsin D could be released by various cell types, including platelets[55], mast cells[56], neutrophils[57], or cytotoxic lymphocytes[58] that are activated under pathological conditions such as hemolysis or coagulation. In addition, Cathepsin D could be released from the degenerated cells of the vessel wall. Along with other factors that might affect blood vessel permeability such as histamine[59], the Cathepsin D and Aβ enriched hemolytic mixture could digest the vasculature and cause enzymatic damage to the blood vessels, which induces further leakage，extracellular matrix digestion and the formation of CAA. When the blood vessel integrity is compromised with leakage or all-out degeneration, the Cathepsin D and Aβ enriched mixture with some invasive ability provided by the proteases entered the brain parenchyma, promoting the formation of senile plaques. Although Cathepsin D could be a very important protease for amyloid aggregation，given the drastic changes and multiple cell types involving hemolysis, vascular degeneration and neuronal inflammation, the participation of multiple proteases such as BACE1[34,35], Cathepsin B[39,40], Carboxypeptidase B[41] or MMP2[42] in this complicate process is possible.

Hemolysis likely also initiates many important molecular interactions in the senile plaques. This study provided both histological and biochemical evidence that Aβ might interact with hemoglobin physically. During hemolysis, with abundant Aβ and hemoglobin, Aβ/Hb ring-shape heterooligomers might be early-stage aggregates in the hemolytic regions. The interaction between Aβ and Hb could be physiologically important as previous research suggested that Aβ binding reduces hemin toxicity[48].

Although Aβ peptides were frequently shown to be cytotoxic to neural cells *in vitro*, since Aβ/Hb complex formation can compete with Aβ self-oligomerization, the possibility of senile plaques serving as Aβ peptide reservoirs to prevent Hb-related toxicity in future hemorrhage events should not be excluded. Our experiment showed that Aβ/Hb complex was sensitive to protease digestion but Aβ self-oligomers were protease resistant, which explains why Aβ stands out as the everlasting and more stable component of senile plaques. The association between ApoE and Aβ was also happening during hemolysis and this association continued to be present in CAA and senile plaques, indicating ApoE is also an early responder to hemolysis and an important component of the senile plaque. The presence of ApoE in the senile plaques has also been reported previously by other research groups[60,61]. In addition, ApoE knockout mice have a strong atherosclerosis phenotype, emphasizing its importance as a blood homeostasis regulator[62-64].

Previous studies in AD patients and in mouse models of AD have already found that dense-core plaques are centered on vessel walls[13,14]. These studies suggested that perturbed vascular transport and/or perivascular enrichment of neuronal Aβ leads to the formation of vasocentric dense plaques. Our results showed that many dense-core plaques are intermingled with degenerated vessel fragments by ColIV, ACTA2 and LRP1 staining, providing further evidence that vascular degeneration is intrinsically linked with senile plaque formation. However, we think that senile plaque Aβ is primarily derived from the blood source although the additional contribution of Aβ from vascular cells or neural cells is possible. A series of studies by Dr. Cullen's group using thick brain tissue sections showed a clear anatomic link between microhemorrhage with senile plaque formation and also Tau phosphorylation[12,17,18]. Yet, in these studies, the exact source of Aβ was still not clear. With Rhodanine staining instead of Perls staining, our study provided a direct link between blood Aβ expression and hemolysis, suggesting that damaged red blood cells were enriched for Aβ. We also established a link between enhanced Aβ staining with vascular damage, which is not surprising since blood cell abnormality is frequently linked with vascular damage. In addition, we

provided biochemical evidence that hemoglobin might form complexes directly with Aβ. In summary, our data suggested that the senile plaque formation is primarily induced by the leakage of hemolytic red blood cells along with other blood contents with CAA and vascular degeneration as intermediate steps. Although amyloid cascade hypothesis is an attractive and straightforward hypothesis as it stands, however, the mechanism of Alzheimer's disease might be much more complicated than previously thought. The AD research field should pay careful attention to the accumulating substantial evidence showing the linkage between senile plaque formation and vascular degeneration and blood abnormalities such as microhemorrhage and hemolysis and be open-minded about revisions on current concepts.

The findings that senile plaques are associated with specific blue autofluorescence are intriguing. There have been a number of studies related to senile plaque blue autofluorescence materials (temporarily named as MetaBlue in this article) in the past[22,23,65]. An early study reported that the blue autofluorescence was associated with senile plaques but not CAA[22]. Two more recent studies found that the blue autofluorescence was associated with both senile plaques and CAA[23,65]. Our study additionally found that MetaBlue was not only associated with CAA and senile plaques but also directly associated with red blood cells. The existence of MetaBlue fluorescence in different kind of senile plaques with different sizes suggests that MetaBlue could be an important component of senile plaques. The exact identity of MetaBlue is unknown. MetaBlue could be an oxidative-stress related metabolite since previous literature indicated that the blue autofluorescence of amyloid peptides could be associated with tyrosine oxidation[66]. To isolate MetaBlue materials and to elucidate the true identity of MetaBlue will likely leads to deeper understanding of AD pathogenesis.

Data and materials availability. All data needed to evaluate the conclusions in this paper are present either in the main text or in the supplementary materials.

872 **Supplementary Materials.**

873 Supplementary Figures 1-4

874

875 **Acknowledgements**: We want to thank the great help from Dr. Ma Chao and Dr. Qiu
876 Wenying for providing AD tissue sections from National Human Brain Bank for
877 Development and Function, Chinese Academy of Medical Sciences and Peking Union
878 Medical College, Beijing, China. Additionally, we want to thank Dr. Xiangli Zhang of
879 Shandong University for valuable discussions. We also want to thank Shunjie Wu from
880 Keyence Co. for allowing us to use their Keyence BZ-X800 microscope without charge.
881 Furthermore, we want to thank Housheng Wang, Lu Xu, Wenting Xuan, Pingxin Liu,
882 Xiaoyi Bao, and Jun Wang for excellent lab assistance. **Funding：** This work was
883 supported by National Natural Science Foundation of China No. 81472235 (H.F.),
884 Shanghai Jiao Tong University Research Grant YG2017MS71 (D.P. and H.F.). **Author**
885 **contributions:** H.F. conceived the study; H. F. designed and supervised the
886 experiments; H.F. and J. L. performed the experiments; H. F., J. L., D.P., W. J., G. G.,
887 D. C. did the data analysis; H. F. wrote the manuscript; All authors reviewed the
888 manuscript. **Competing interests:** Authors declare no competing interests.

889

890 **References:**

891

892 1 Lane, C. A., Hardy, J. & Schott, J. M. Alzheimer's disease. *Eur J Neurol* **25**, 59-70,
893 doi:10.1111/ene.13439 (2018).
894 2 Attems, J., Lintner, F. & Jellinger, K. A. Amyloid beta peptide 1-42 highly correlates with capillary
895 cerebral amyloid angiopathy and Alzheimer disease pathology. *Acta neuropathologica* **107**,
896 283-291, doi:10.1007/s00401-004-0822-6 (2004).
897 3 van Helmond, Z., Miners, J. S., Kehoe, P. G. & Love, S. Oligomeric Abeta in Alzheimer's disease:
898 relationship to plaque and tangle pathology, APOE genotype and cerebral amyloid angiopathy.
899 *Brain Pathol* **20**, 468-480, doi:10.1111/j.1750-3639.2009.00321.x (2010).
900 4 Glenner, G. G., Henry, J. H. & Fujihara, S. Congophilic angiopathy in the pathogenesis of
901 Alzheimer's degeneration. *Annales de pathologie* **1**, 120-129 (1981).
902 5 Glenner, G. G. & Wong, C. W. Alzheimer's disease: initial report of the purification and
903 characterization of a novel cerebrovascular amyloid protein. *Biochemical and biophysical*
904 *research communications* **120**, 885-890, doi:10.1016/s0006-291x(84)80190-4 (1984).
905 6 Masters, C. L. *et al.* Amyloid plaque core protein in Alzheimer disease and Down syndrome.

Proceedings of the National Academy of Sciences of the United States of America **82**, 4245-4249, doi:10.1073/pnas.82.12.4245 (1985).

7 Hardy, J. A. & Higgins, G. A. Alzheimer's disease: the amyloid cascade hypothesis. *Science* **256**, 184-185, doi:10.1126/science.1566067 (1992).

8 Hardy, J. Alzheimer's disease: the amyloid cascade hypothesis: an update and reappraisal. *Journal of Alzheimer's disease : JAD* **9**, 151-153, doi:10.3233/jad-2006-9s317 (2006).

9 Miyakawa, T., Shimoji, A., Kuramoto, R. & Higuchi, Y. The relationship between senile plaques and cerebral blood vessels in Alzheimer's disease and senile dementia. Morphological mechanism of senile plaque production. *Virchows Archiv. B, Cell pathology including molecular pathology* **40**, 121-129, doi:10.1007/bf02932857 (1982).

10 Kawai, M., Kalaria, R. N., Harik, S. I. & Perry, G. The relationship of amyloid plaques to cerebral capillaries in Alzheimer's disease. *The American journal of pathology* **137**, 1435-1446 (1990).

11 Sparks, D. L., Kuo, Y. M., Roher, A., Martin, T. & Lukas, R. J. Alterations of Alzheimer's disease in the cholesterol-fed rabbit, including vascular inflammation. Preliminary observations. *Annals of the New York Academy of Sciences* **903**, 335-344, doi:10.1111/j.1749-6632.2000.tb06384.x (2000).

12 Cullen, K. M., Kocsi, Z. & Stone, J. Microvascular pathology in the aging human brain: Evidence that senile plaques are sites of microhaemorrhages. *Neurobiol Aging* **27**, 1786-1796, doi:10.1016/j.neurobiolaging.2005.10.016 (2006).

13 Kumar-Singh, S. *et al.* Dense-core senile plaques in the Flemish variant of Alzheimer's disease are vasocentric. *The American journal of pathology* **161**, 507-520, doi:10.1016/S0002-9440(10)64207-1 (2002).

14 Kumar-Singh, S. *et al.* Dense-core plaques in Tg2576 and PSAPP mouse models of Alzheimer's disease are centered on vessel walls. *The American journal of pathology* **167**, 527-543, doi:10.1016/S0002-9440(10)62995-1 (2005).

15 Bu, X. L. *et al.* Blood-derived amyloid-beta protein induces Alzheimer's disease pathologies. *Molecular psychiatry* **23**, 1948-1956, doi:10.1038/mp.2017.204 (2018).

16 Ryu, J. K. & McLarnon, J. G. A leaky blood-brain barrier, fibrinogen infiltration and microglial reactivity in inflamed Alzheimer's disease brain. *Journal of cellular and molecular medicine* **13**, 2911-2925, doi:10.1111/j.1582-4934.2008.00434.x (2009).

17 Cullen, K. M., Kócsi, Z. & Stone, J. Pericapillary Haem-Rich Deposits: Evidence for Microhaemorrhages in Aging Human Cerebral Cortex. *Journal of Cerebral Blood Flow & Metabolism* **25**, 1656-1667, doi:10.1038/sj.jcbfm.9600155 (2005).

18 Hansra, G. K. *et al.* The neuritic plaque in Alzheimer's disease: perivascular degeneration of neuronal processes. *Neurobiol Aging* **82**, 88-101, doi:https://doi.org/10.1016/j.neurobiolaging.2019.06.009 (2019).

19 Sun, H. L. *et al.* Blood cell-produced amyloid-beta induces cerebral Alzheimer-type pathologies and behavioral deficits. *Mol Psychiatr*, doi:10.1038/s41380-020-0842-1 (2020).

20 Fu, H. *et al.* Persisting and Increasing Neutrophil Infiltration Associates with Gastric Carcinogenesis and E-cadherin Downregulation. *Scientific reports* **6**, 29762, doi:10.1038/srep29762 (2016).

21 Wallin, C., Luo, J. H., Jarvet, J., Warmlander, S. K. T. S. & Graslund, A. The Amyloid-beta Peptide in Amyloid Formation Processes: Interactions with Blood Proteins and Naturally Occurring Metal Ions. *Isr J Chem* **57**, 674-685, doi:10.1002/ijch.201600105 (2017).

22 Dowson, J. H. A sensitive method for the demonstration of senile plaques in the dementing brain. *Histopathology* **5**, 305-310, doi:10.1111/j.1365-2559.1981.tb01789.x (1981).

23 Gao, Y. *et al.* Imaging and Spectral Characteristics of Amyloid Plaque Autofluorescence in Brain Slices from the APP/PS1 Mouse Model of Alzheimer's Disease. *Neuroscience bulletin* **35**, 1126-1137, doi:10.1007/s12264-019-00393-6 (2019).

24 Cohen, R. M. *et al.* Red cell life span heterogeneity in hematologically normal people is sufficient to alter HbA1c. *Blood* **112**, 4284-4291, doi:10.1182/blood-2008-04-154112 (2008).

25 Holtzman, D. M. Role of apoE/A beta interactions in the pathogenesis of Alzheimer's disease and cerebral amyloid angiopathy. *J. Mol. Neurosci.* **17**, 147-155, doi:10.1385/jmn:17:2:147 (2001).

26 Li, Q. X. *et al.* Membrane-associated forms of the beta A4 amyloid protein precursor of Alzheimer's disease in human platelet and brain: surface expression on the activated human platelet. *Blood* **84**, 133-142 (1994).

27 Koupenova, M., Kehrel, B. E., Corkrey, H. A. & Freedman, J. E. Thrombosis and platelets: an update. *European heart journal* **38**, 785-791, doi:10.1093/eurheartj/ehw550 (2017).

28 Ferguson, D. J. Acute intravascular hemolysis after a platelet transfusion. *CMAJ : Canadian Medical Association journal = journal de l'Association medicale canadienne* **138**, 523-524 (1988).

29 Weinstein, L. Syndrome of hemolysis, elevated liver enzymes, and low platelet count: A severe consequence of hypertension in pregnancy. *Am J Obstet Gynecol* **193**, 859-860, doi:10.1016/j.ajog.2005.02.113 (2005).

30 Helms, C. C. *et al.* Mechanisms of hemolysis-associated platelet activation. *Journal of Thrombosis and Haemostasis* **11**, 2148-2154, doi:10.1111/jth.12422 (2013).

31 Scheibel, A. B. Alterations of the cerebral capillary bed in the senile dementia of Alzheimer. *The Italian Journal of Neurological Sciences* **8**, 457-463, doi:10.1007/bf02334602 (1987).

32 Bu, G., Cam, J. & Zerbinatti, C. LRP in amyloid-beta production and metabolism. *Ann N Y Acad Sci*, 005 (2006).

33 Storck, S. E. *et al.* Endothelial LRP1 transports amyloid-beta(1-42) across the blood-brain barrier. *J. Clin. Invest.* **126**, 123-136, doi:10.1172/jci81108 (2016).

34 Yan, R. *et al.* Membrane-anchored aspartyl protease with Alzheimer's disease β-secretase activity. *Nature* **402**, 533-537, doi:10.1038/990107 (1999).

35 Cai, H. *et al.* BACE1 is the major β-secretase for generation of Aβ peptides by neurons. *Nature Neuroscience* **4**, 233-234, doi:10.1038/85064 (2001).

36 Chevallier, N. *et al.* Cathepsin D displays in vitro beta-secretase-like specificity. *Brain Res.* **750**, 11-19, doi:10.1016/s0006-8993(96)01330-3 (1997).

37 Schechter, I. & Ziv, E. Kinetic properties of cathepsin D and BACE 1 indicate the need to search for additional beta-secretase candidate(s). *Biol. Chem.* **389**, 313-320, doi:10.1515/bc.2008.025 (2008).

38 Evin, G. *et al.* Candidate gamma-secretases in the generation of the carboxyl terminus of the Alzheimer's disease beta-A4 amyloid: Possible involvement of cathepsin D. *Biochemistry* **34**, 14185-14192, doi:10.1021/bi00043a024 (1995).

39 Schechter, I. & Ziv, E. Cathepsins S, B and L with aminopeptidases display β-secretase activity associated with the pathogenesis of Alzheimer's disease. **392**, 555-569, doi:doi:10.1515/bc.2011.054 (2011).

40 Hook, V. Y. H., Kindy, M., Reinheckel, T., Peters, C. & Hook, G. Genetic cathepsin B deficiency reduces beta-amyloid in transgenic mice expressing human wild-type amyloid precursor protein. *Biochem. Biophys. Res. Commun.* **386**, 284-288, doi:10.1016/j.bbrc.2009.05.131 (2009).

41 Matsumoto, A., Itoh, K. & Matsumoto, R. A novel carboxypeptidase B that processes native beta-amyloid precursor protein is present in human hippocampus. *Eur. J. Neurosci.* **12**, 227-238, doi:10.1046/j.1460-9568.2000.00908.x (2000).

42 Lepage, R. N. *et al.* Gelatinase A possesses a beta-secretase-like activity in cleaving the amyloid protein precursor of Alzheimer's disease. *FEBS Letters* **377**, 267-270, doi:10.1016/0014-5793(95)01358-x (1995).

43 Papassotiropoulos, A. *et al.* Genetic polymorphism of cathepsin D is strongly associated with the risk for developing sporadic Alzheimer's disease. *Neuroscience Letters* **262**, 171-174, doi:https://doi.org/10.1016/S0304-3940(99)00071-3 (1999).

44 Schuur, M. *et al.* Cathepsin D gene and the risk of Alzheimer's disease: A population-based study and meta-analysis. *Neurobiology of Aging* **32**, 1607-1614, doi:https://doi.org/10.1016/j.neurobiolaging.2009.10.011 (2011).

45 Bernstein, H. G., Bruszis, S., Schmidt, D., Wiederanders, B. & Dorn, A. Immunodetection of cathepsin D in neuritic plaques found in brains of patients with dementia of Alzheimer type. *Journal fur Hirnforschung* **30**, 613-618 (1989).

46 Cataldo, A. M., Barnett, J. L., Mann, D. M. A. & Nixon, R. A. Colocalization of Lysosomal Hydrolase and β-Amyloid in Diffuse Plaques of the Cerebellum and Striatum in Alzheimer's Disease and Down's Syndrome. *Journal of Neuropathology & Experimental Neurology* **55**, 704-715, doi:10.1097/00005072-199606000-00004 (1996).

47 Wu, C. W. *et al.* Hemoglobin promotes Abeta oligomer formation and localizes in neurons and amyloid deposits. *Neurobiology of disease* **17**, 367-377, doi:10.1016/j.nbd.2004.08.014 (2004).

48 Chuang, J. Y. *et al.* Interactions between amyloid-beta and hemoglobin: implications for amyloid plaque formation in Alzheimer's disease. *PloS one* **7**, e33120, doi:10.1371/journal.pone.0033120 (2012).

49 Howlett, D., Cutler, P., Heales, S. & Camilleri, P. Hemin and related porphyrins inhibit beta-amyloid aggregation. *FEBS letters* **417**, 249-251 (1997).

50 Liu, Y. *et al.* Hemin as a generic and potent protein misfolding inhibitor. *Biochemical and biophysical research communications* **454**, 295-300, doi:10.1016/j.bbrc.2014.10.062 (2014).

51 de la Torre, J. C. & Aliev, G. Alzheimer's disease is a vascular disorder with neurodegenerative consequences. *J Neurol Sci* **229**, 305-306 (2005).

52 Smith, R. P. & Broze, G. J., Jr. Characterization of platelet-releasable forms of beta-amyloid precursor proteins: the effect of thrombin. *Blood* **80**, 2252-2260 (1992).

53 Van Nostrand, W. E., Schmaier, A. H., Farrow, J. S. & Cunningham, D. D. Platelet protease nexin-2/amyloid beta-protein precursor. Possible pathologic and physiologic functions. *Annals of the New York Academy of Sciences* **640**, 140-144, doi:10.1111/j.1749-6632.1991.tb00205.x (1991).

54 Canobbio, I. *et al.* Platelet amyloid precursor protein is a modulator of venous thromboembolism in mice. *Blood* **130**, 527-536, doi:10.1182/blood-2017-01-764910 (2017).

55 Rendu, F. & Brohard-Bohn, B. The platelet release reaction: granules' constituents, secretion and functions. *Platelets* **12**, 261-273, doi:10.1080/09537100120068170 (2001).

56 Puri, N. & Roche, P. A. Mast cells possess distinct secretory granule subsets whose exocytosis

is regulated by different SNARE isoforms. *Proc Natl Acad Sci U S A* **105**, 2580-2585 (2008).

57 Conus, S. *et al.* Caspase-8 is activated by cathepsin D initiating neutrophil apoptosis during the resolution of inflammation. *J Exp Med* **205**, 685-698 (2008).

58 Burkhardt, J. K., Hester, S., Lapham, C. K. & Argon, Y. The lytic granules of natural killer cells are dual-function organelles combining secretory and pre-lysosomal compartments. *The Journal of cell biology* **111**, 2327-2340, doi:10.1083/jcb.111.6.2327 (1990).

59 Sedeyn, J. C. *et al.* Histamine Induces Alzheimer's Disease-Like Blood Brain Barrier Breach and Local Cellular Responses in Mouse Brain Organotypic Cultures. *Biomed Res Int* **937148**, 30 (2015).

60 Namba, Y., Tomonaga, M., Kawasaki, H., Otomo, E. & Ikeda, K. Apolipoprotein E immunoreactivity in cerebral amyloid deposits and neurofibrillary tangles in Alzheimer's disease and kuru plaque amyloid in Creutzfeldt-Jakob disease. *Brain Res.* **541**, 163-166, doi:https://doi.org/10.1016/0006-8993(91)91092-F (1991).

61 Wisniewski, T. & Frangione, B. Apolipoprotein E: A pathological chaperone protein in patients with cerebral and systemic amyloid. *Neuroscience Letters* **135**, 235-238, doi:https://doi.org/10.1016/0304-3940(92)90444-C (1992).

62 Nakashima, Y., Plump, A. S., Raines, E. W., Breslow, J. L. & Ross, R. ApoE-deficient mice develop lesions of all phases of atherosclerosis throughout the arterial tree. *Arteriosclerosis and Thrombosis* **14**, 133-140, doi:10.1161/01.atv.14.1.133 (1994).

63 Seo, H. S. *et al.* Peripheral vascular stenosis in apolipoprotein E-deficient mice. Potential roles of lipid deposition, medial atrophy, and adventitial inflammation. *Arterioscler Thromb Vasc Biol* **17**, 3593-3601 (1997).

64 Rosenfeld, M. E. *et al.* Advanced atherosclerotic lesions in the innominate artery of the ApoE knockout mouse. *Arterioscler Thromb Vasc Biol* **20**, 2587-2592 (2000).

65 Kwan, A. C., Duff, K., Gouras, G. K. & Webb, W. W. Optical visualization of Alzheimer's pathology via multiphoton-excited intrinsic fluorescence and second harmonic generation. *Opt Express* **17**, 3679-3689, doi:10.1364/Oe.17.003679 (2009).

66 Fricano, A., Librizzi, F., Rao, E., Alfano, C. & Vetri, V. Blue autofluorescence in protein aggregates "lighted on" by UV induced oxidation. *Biochimica et biophysica acta. Proteins and proteomics* **1867**, 140258, doi:10.1016/j.bbapap.2019.07.011 (2019).

Supplementary Information for

Senile plaques arise from Cathepsin D and Aβ-enriched proteinaceous mixtures out of hemolysis and vascular degeneration

Hualin Fu, Jilong Li, Peng Du, Weilin Jin, Guo Gao, Daxiang Cui

This PDF file includes:

Supplementary Fig. 1 to 4

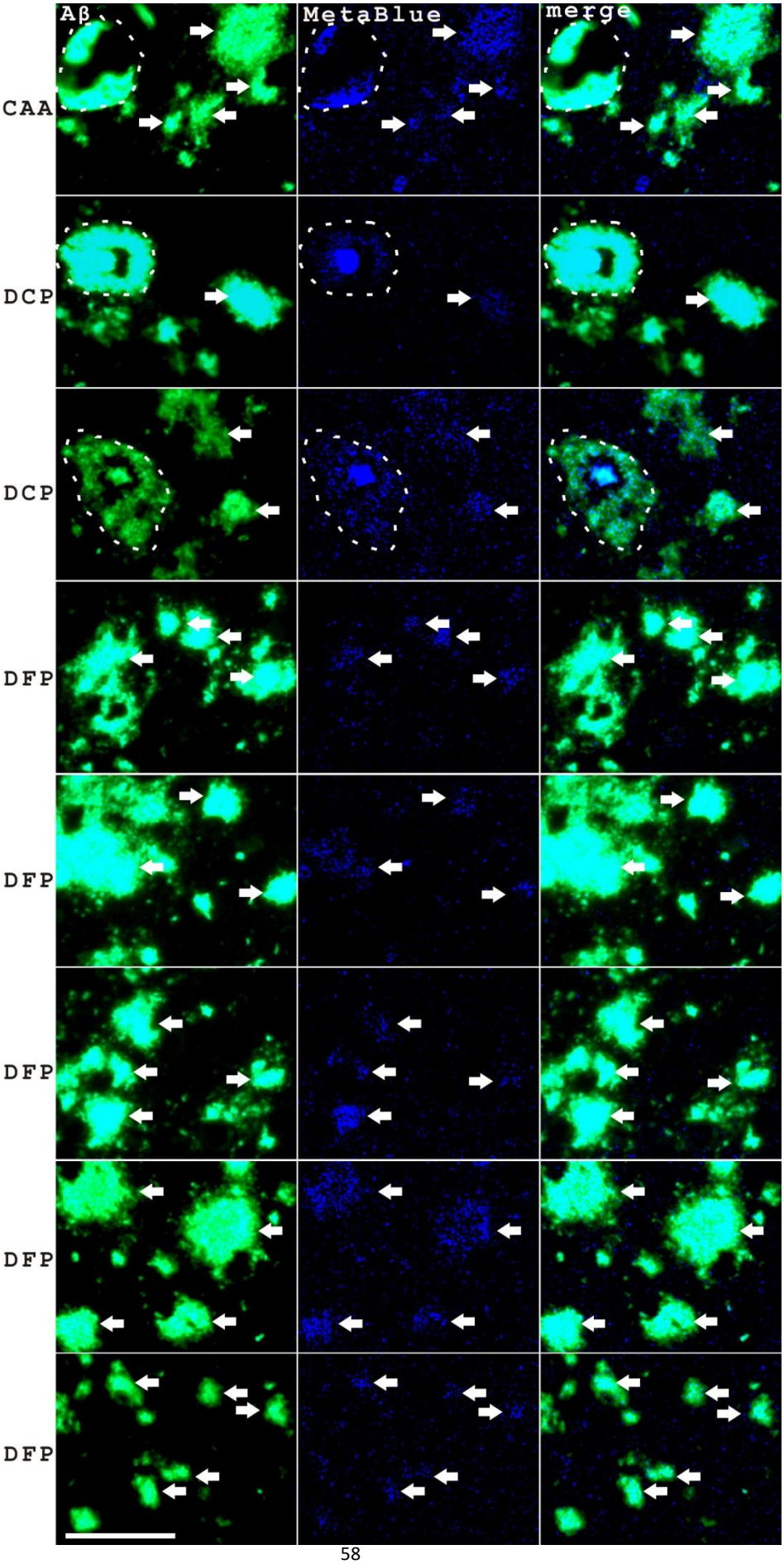

1082

Supplementary Figure 1. MetaBlue is a robust and consistent marker of senile plaques. MetaBlue and Aβ staining in CAA (top panel), dense-core plaques (second and third panels, DCP) and in diffusive plaques (bottom five panels, DFP) was shown in this figure. Dashed lines indicated CAA or dense-core plaques while the arrows indicated diffusive plaques. Scale bar, 50 μm.

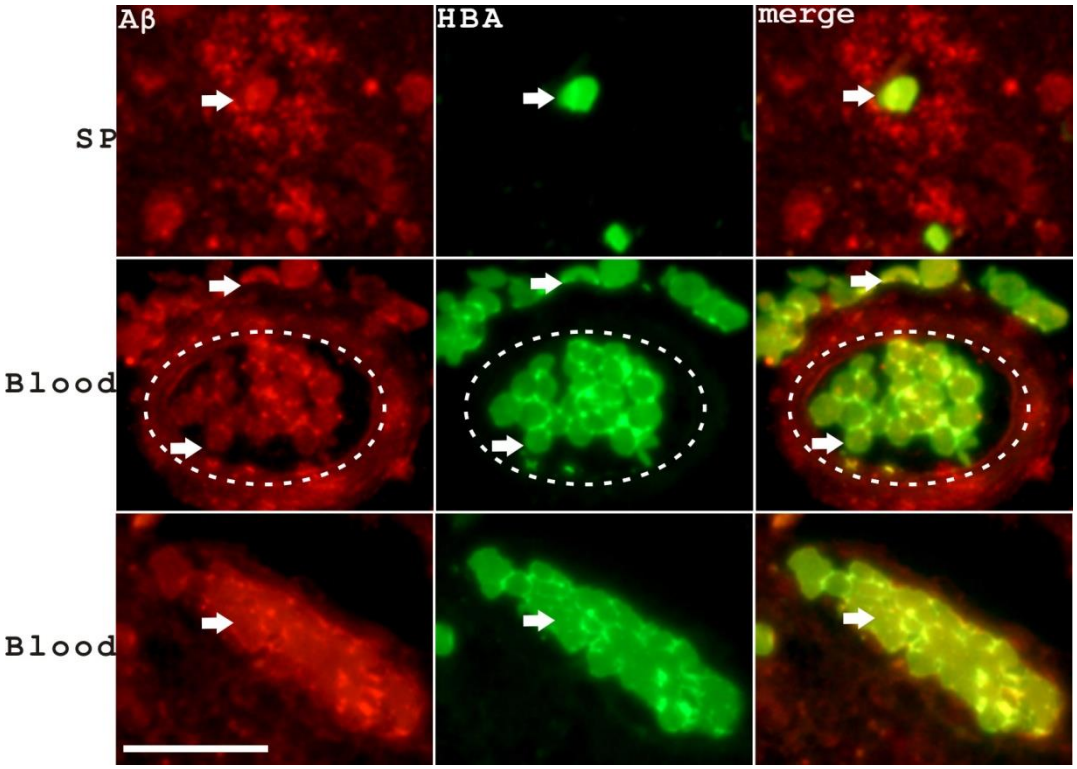

Supplementary Figure 2. The co-expression of Aβ and red blood cell marker alpha hemoglobin (HBA). Aβ staining of a single red blood cell marked with HBA in the center of a senile plaque was shown in the top panel. Aβ staining of red blood cells marked with HBA during red blood cell extravasation was shown in the middle panel. Aβ staining of red blood cells marked with HBA during intravascular hemolysis with the disappearance of clear round shape structure of red blood cells was shown at the bottom. The arrow indicated Aβ and HBA co-staining. The dashed lines indicated the outline of a blood vessel. Scale bar, 50 μm.

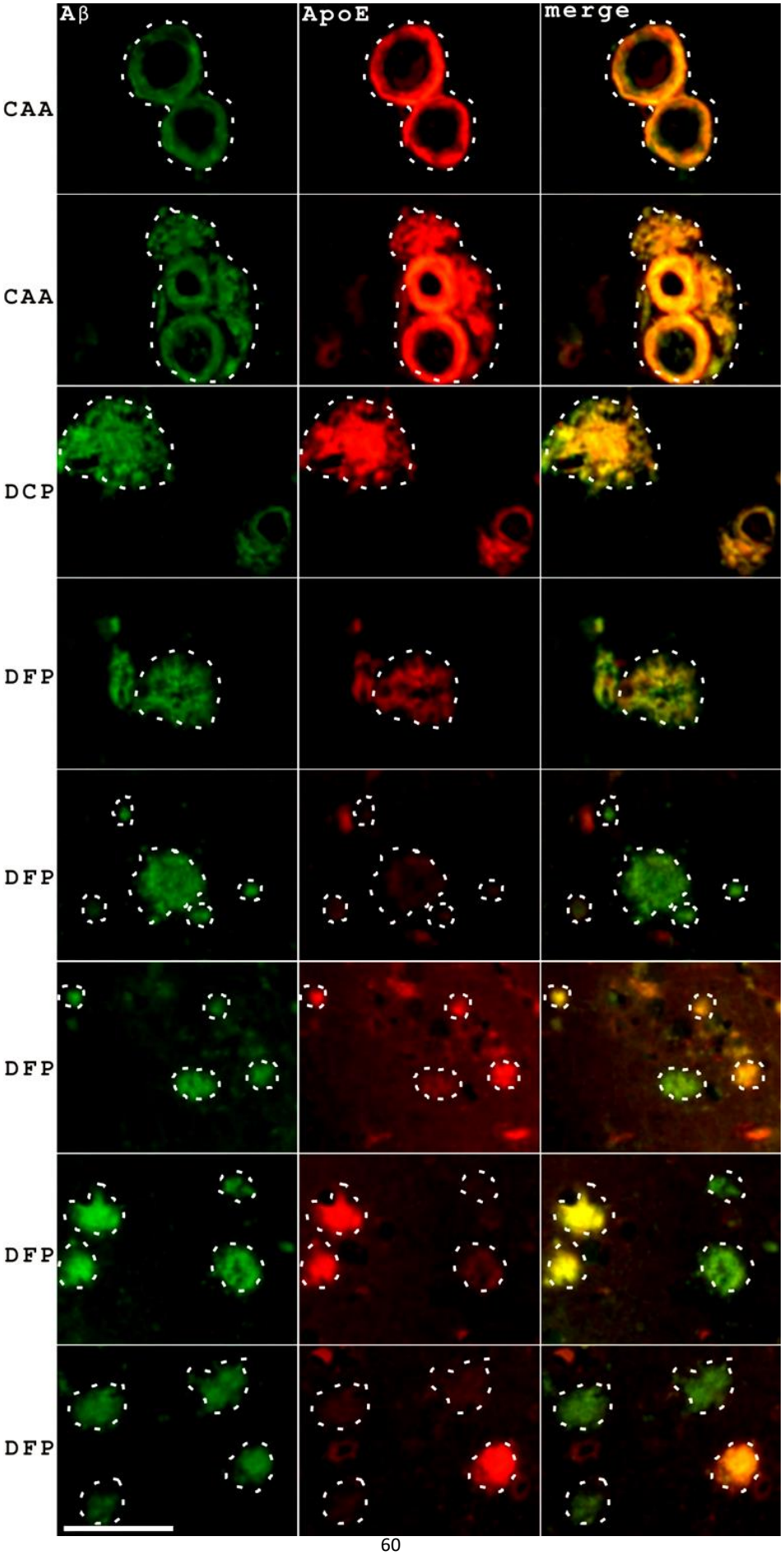

1099

Supplementary Figure 3. ApoE is a constitutive component of senile plaques. ApoE and Aβ staining in CAA (dashed lines, top two panels) and in a dense-core senile plaque (dashed lines, third panel) and in diffusive senile plaques (dashed lines, bottom five panels) was shown in this figure. ApoE and Aβ staining in diffusive senile plaques with different sizes showed highly variable ApoE intensities. Scale bar, 50 μm.

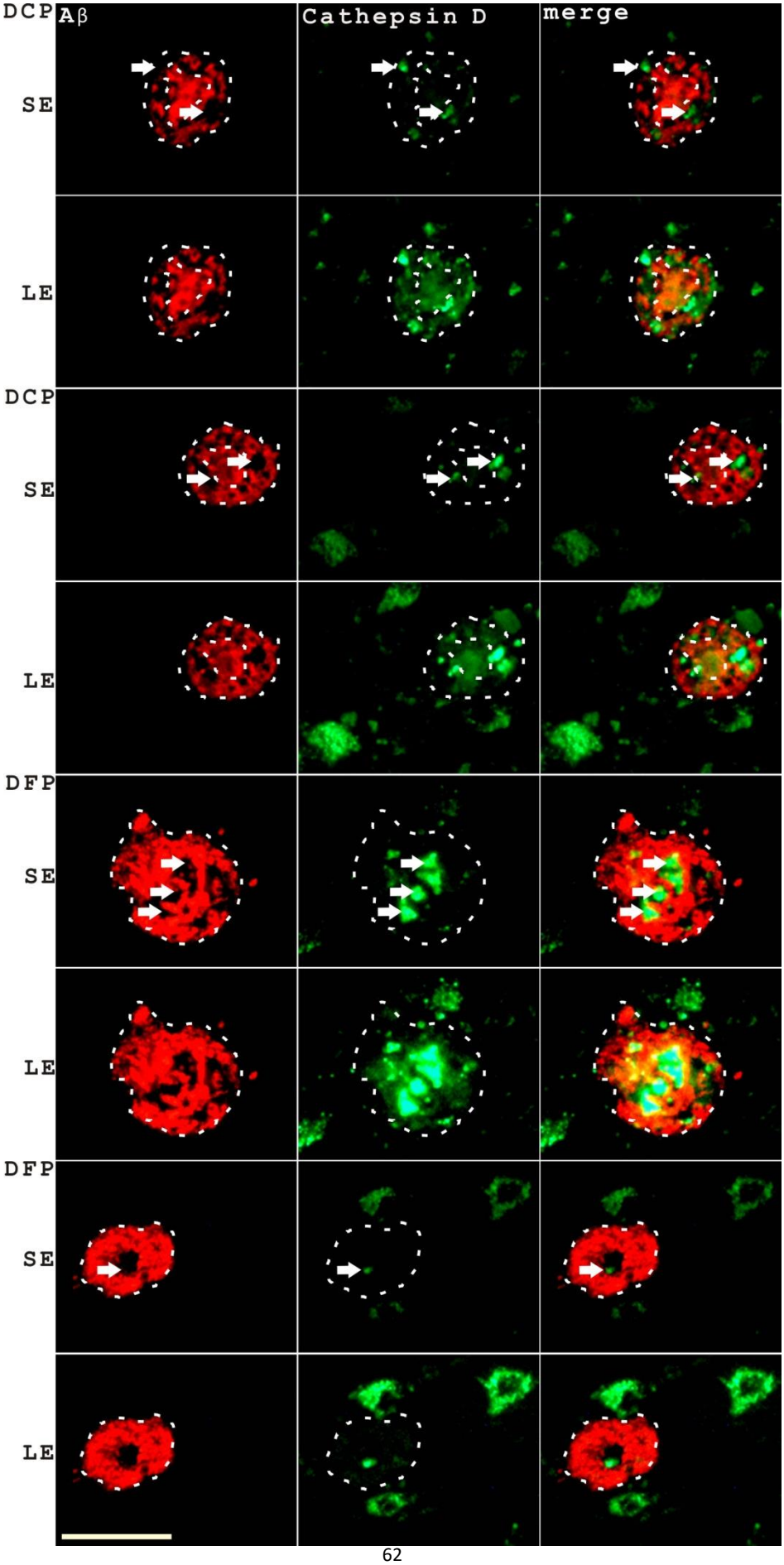

1110

Supplementary Figure 4. The two distinct layers of Cathepsin D expression in senile plaques were verified with another Aβ/Cathepsin D antibody pair. Dense-core senile plaques showed two layers of Cathepsin D staining using two different exposure setting of the Cathepsin D staining were shown in the top four panels (SE stands for short exposure of 0.5 second while LE stands for long exposure of 1 second). A diffusive senile plaque with two layers of Cathepsin D staining was shown in the fifth and sixth panels. A diffusive senile plaque with very weak plaque Aβ-overlapping Cathepsin D staining was shown in the bottom two panels. The arrows pointed to the strong granule type of Cathepsin D staining while the dashed lines indicated the weaker but constitutive Cathepsin D staining overlapping with senile plaque Aβ staining. Scale bar, 50 μm.